Pheromone-dependent olfaction bidirectionally regulates muscle extracellular vesicles formation

Katarzyna Banasiak[1], Agata Szczepańska[2], Klaudia Kołodziejska[2], Abdulrahman Tudu Ibrahim[2,3], Wojciech Pokrzywa[1*], Michał Turek[2*]

Affiliations:

[1]*Laboratory of Protein Metabolism, International Institute of Molecular and Cell Biology in Warsaw, Poland.*

[2]*Laboratory of Animal Molecular Physiology, Institute of Biochemistry and Biophysics, Polish Academy of Sciences, Warsaw, Poland*

[3]*Faculty of Chemistry, Warsaw University of Technology, Warsaw, Poland*

* Co-corresponding authors

Correspondence should be directed to:

MT: m.turek@ibb.waw.pl

WP: wpokrzywa@iimcb.gov.pl

Abstract

Extracellular vesicles (EVs), entities transporting a variety of cargo, are directly involved in many biological processes and intercellular communication, the characterization of which

requires studying multi-tissue organisms. We previously demonstrated that the largest evolutionarily conserved EVs, exophers, are a component of the *C. elegans* maternal somatic tissue resource management system, and their formation is induced by the embryos developing *in utero*. In this study, we explored inter-tissue regulatory networks of exophergenesis. We found that exophergenesis activity is differentially modulated by sex-specific ascaroside (pheromones) signaling molecules, known to have multiple functions in development and behavior. While hermaphrodite-released pheromones down-regulate exophergenesis, male-released pheromones favor strong exopher production. This ascaroside-dependent regulation is fine-tuned by exopher-promoting olfactory neurons exposed to the environment and exopher-inhibiting sensory neurons exposed to the body cavity. Therefore, we uncovered critical control nodes for muscle exophergenesis in response to environmental and internal conditions. Our findings may imply the existence of an analogous mechanism regulating cardiomyocyte exophers, which contributes to the olfactory dysfunction-dependent risk of cardiovascular disease in humans.

Keywords

C. elegans, muscles, extracellular vesicles, exophers, pheromones, olfactory neurons

Main

Extracellular vesicles (EVs) are lipid-bilayer-enclosed particles that most cell types release. Two major EV types can be distinguished based on their biogenesis: endosome-derived exosomes and membrane-derived ectosomes[1]. EVs can be employed by cells to remove unwanted biological material, such as misfolded proteins and damaged organelles, or to transport small molecules, including proteins and nucleic acids, enabling exchange and communication between cells. Therefore, they are critical in physiological processes and

pathological states involving disrupted cellular homeostasis[2–5]. To study EVs' genesis, content, and function, multicellular animal models are frequently employed. The nematode *C. elegans* has been successfully used to investigate the biology of EVs generated by various tissues, including neurons[6,7], muscles[8], hypodermis[9], and reproductive system[10,11]. Here, as a model, we use a class of recently discovered EVs, termed exophers, to understand how ectosome biogenesis in somatic tissue is regulated at the whole organism level employing worms. Exophergenesis (i.e., exopher generation) is an evolutionarily conserved phenomenon found from invertebrates to mammals, including humans. Exophers were shown to play a significant role in cellular stress response, tissue homeostasis, and organismal reproduction[7,8,12,13]. It was demonstrated that *C. elegans* neurons retain their regular activity in the face of proteotoxic stress by expelling protein aggregates, damaged mitochondria, and lysosomes into surrounding tissues via exophers[7]. Nicolás-Ávila et al. also demonstrated that mouse cardiomyocytes excrete defective mitochondria via exophers, which, in turn, restricts waste accumulation in the extracellular space and inflammasome activation, promoting metabolic homeostasis in the heart[13]. However, the biological roles of exophers extend beyond the elimination of superfluous cellular components. In our previous work, we showed that the body wall muscles (BWM) of *C. elegans* release exophers that can transport muscle-synthesized yolk proteins to support offspring development, increasing their odds of adapting to environmental conditions[8]. We do not, however, comprehend the mechanism of cell non-autonomous regulation of muscle exophergenesis nor how this maternal somatic tissue resource management system responds to environmental conditions.

Animal-to-animal signals transmitted by pheromones in *C. elegans* have been shown to regulate maternal provisioning, development, and generation time [14–16]. Since muscle exophers mediate the transfer of maternal resources to offspring supporting their development, we hypothesized that exophergenesis (Fig. 1a) is regulated by metabolites-mediated social cues

generated within the worm population. To investigate this, we cultured hermaphrodites on plates under two conditions and quantified exopher production by BWM. As the first condition, we used hermaphrodites cultured individually on a plate, thereby eliminating social cues from other worms. As a second condition, we used worms raised in a ten-hermaphrodites population from the beginning of their development (Fig. 1b). We noted that animals grown together in a ten-hermaphrodite population released, on average, 44% fewer exophers than single-grown worms (Fig. 1c). Hermaphrodites from both experimental groups contain the same number of embryos in utero (Fig. 1d), demonstrating that signaling from other hermaphrodites can modulate exopher production independently from previously postulated embryo-maternal signaling[8]. Moreover, growing hermaphrodites on plates with different population densities indicate a dose-dependent effect (Extended Data Fig. 1a). To rule out the possibility that exophergenesis is substantially regulated by the molecules derived from the bacterial food source, which could indirectly influence animal to animal communication, we decided to test various bacterial strains effect on worm's muscle exopher production. We directly compared *Escherichia coli* B strain OP50 and K-12 strain HT115, which are widely used in *C. elegans* culture[17] and RNAi silencing experiments[18], respectively. As a result, we observed a slight increase in exopher number upon the *E. coli* HT115 diet compared to the OP50 diet (Extended Data Fig. 1b). However, the number of eggs present *in utero* at adulthood day 2 was elevated upon the HT115 diet (Extended Data Fig. 1c). Whether or not the bacteria were metabolically active (PFA-killed prior to plate culture) was irrelevant (Extended Data Fig. 1b), confirming that exophergenesis is robustly activated in worm's muscles regardless of the bacteria type used as a food source.

Next, we investigated if the presence of males influences exophers production by hermaphrodites similarly to the presence of other hermaphrodites. To verify this, we monitored the number of exophers in *him-5* mutants characterized by a significant increase of males in

the population (about 33% compared to 0.3% for wild type)[19]. Interestingly, *him-5* animals grown with males until the L4 stage and then transferred to a male-free plate (Fig. 1e) produce approximately 2.5 times more exophers than wild-type hermaphrodites grown from L1 on a male-free plate (Fig. 1f). This increase appears to be mediated by the embryo-maternal signaling as *him-5* mutant hermaphrodites contain 26% more embryos *in utero* than wild-type hermaphrodites (Fig. 1g). To rule out the possibility that an increase in the number of exophers released, may be a result of the *him-5* mutation rather than the presence of males in the population, we grew wild-type hermaphrodites on a plate conditioned with males for 48 hours, which we then removed (Fig. 1h). Growing hermaphrodites on male-conditioned plates increased exopher production to the same degree as when hermaphrodites were grown with males until the L4 larvae stage (Fig. 1i), regardless of the bacteria strain used as a food source (Extended Data Fig. 1d). However, this increase in exophers production was associated with a rise in the number of *in utero* embryos (Fig. 1j), indicating that *C. elegans* male pheromones can also drive embryo retention in hermaphrodite's uterus. Furthermore, adult hermaphrodites exposed to males' secretions as larvae showed no further increase in exopher production (Extended Data Fig. 1e). Our data indicate that exophers generation by hermaphrodite BWM is modulated by signals released in response to pheromonal stimulation. Male pheromones act through embryo-maternal signaling, while pheromones released by hermaphrodites downregulate exophergenesis independently from this pathway.

To further investigate muscle exopher regulation by pheromones, we took advantage of several worm mutants with altered ascaroside pheromones side-chain biosynthesis[20] (Fig. 2a). Mutants of the *maoc-1* gene display a reduction in exopher production, whereas the *daf-22* and *acox-1* mutants show an increase in exopher production (Fig. 2b). However, changes in exophergenesis levels in mutants correlate with the number of embryos present in their uterus (Fig. 2c), therefore, could be dependent on the embryo-maternal signaling. To distinguish the

change in exopher production from embryo-maternal signaling in the mutants mentioned above, we examined exophergenesis in wild-type animals maintained on plates with ascaroside biosynthesis mutants (one wild-type worm with nine mutant worms per plate) (Fig. 2d). The number of embryos in the uterus of wild-type animals reared in this way did not change (Fig. 2f), yet we observed a decrease in exophergenesis in wild-type worms grown together with *maoc-1* mutants and an increase in the presence of *acox-1* worms (Fig. 2e). Finally, we isolated *C. elegans* secretory products from starving N2 wild-type and *maoc-1* mutant populations as previously described[21]. Next, we exposed growing worms to this isolate (Fig. 2g), which led to the increase in exophergenesis in a *maoc-1*-dependent manner (Fig. 2h). These results further confirm pheromone-based regulation of exopher formation with a critical role for ascarosides whose synthesis is mediated by MAOC-1.

Since many olfactory neurons detect ascarosides[22] (Fig. 3a), we examined whether genetic ablation of all ciliated sensory neurons would abolish pheromone-regulated exopher induction. Indeed, as shown in Fig. 3b, *che-13* mutants, which do not form proper cilia and are incapable of pheromone detection[23], produce a minimal number of exophers. Furthermore, exposure of the *che-13* mutant to metabolites secreted by starving wild-type worms did not affect exopher production (Fig. 3c). To determine which sensory neurons mediate pheromone-dependent modulation of exophergenesis, we examined its level in animals with genetically ablated sensory neurons previously shown to be capable of pheromone detection[22]. The removal of ASK, ADL, or AWC neurons inhibited exopher production comparable to that observed in *che-13* mutants, whereas the ablation of ASH led to a slight decrease in exophergenesis. Notably, hermaphrodites with the addition of male-specific, pheromone-sensing CEM neurons (via *ceh-30* gain-of-function mutation[24]) did not show alterations in exopher production (Fig. 3d).

To identify neurons critical for the exophergenesis downregulation in response to the presence of other hermaphrodites, we grew hermaphrodites with genetic ablations of different classes of

olfactory neurons either as a single animal or in a ten-worms population (Fig. 1b scheme). Our analyses using mutant strains with impaired olfaction showed that ASH and ASI neurons play a crucial role in exophergenesis, with a small modulation coming from ASK neurons (Fig. 3e). Finally, masculinization of a hermaphrodite olfactory circuit by the addition of CEM male-specific neurons leads to a decrease in exopher production in solitary animals (Fig. 3e).

Next, we investigated which olfactory neurons are necessary to detect male pheromones responsible for exophergenesis upregulation. To this end, we grew hermaphrodites with genetic ablations of different classes of olfactory neurons on male-conditioned plates (as shown in Fig. 1h scheme). Our results demonstrate that the removal of ASK, AWB, or ADL neurons abolishes an increase in exopher production induced by male-released pheromones (Fig. 3f). These results align with previously described roles for ASK, AWB, and ADL neurons in male pheromones sensing[25–28].

Since genetic ablation of AWC thermo-responsive neurons[29,30] has a prominent effect on exophergenesis (Fig. 3d), we also investigated whether this process could be temperature-dependent. To assess this, we grew worms at 15, 20, or 25°C and measured the number of exophers produced by hermaphrodites that were at the peak of progeny production for each temperature[31]. We observed that the generation of muscle exophers increased as worm incubation temperature rises (Fig. 3g). Moreover, the removal of AWC aggravates this response, demonstrating temperature-dependent regulation of exophergenesis by these neurons (Fig. 3g).

The binding of signaling molecules to the relevant receptor is the first step in transducing neuron chemosensory signals. More than 1,300 G protein-coupled receptors (GPCRs) mediate this communication in *C. elegans*[32]. Internal states and environmental conditions can modulate GPCRs expression to affect worm behavior[33–36]. To identify the receptor(s) responsible for ascaroside-mediated alterations in exopher formation, we performed RNA-sequencing of

animals grown either as a single animal or in a ten-hermaphrodites population (Extended Data Fig. 2a). On the transcriptional level, neither group differed markedly (Extended Data Fig. 2b), and none of the 7TM receptors was significantly up- or down-regulated (Supplementary Table 1). However, *str-173* receptor transcript, which shows among all of the 7TM receptors one of the most evident trends between growth conditions (2.3 fold change) is, according to single-cell RNA-seq data[37], expressed almost exclusively in ASK neurons (Extended Data Fig. 2c). Since ASK is crucial for pheromone-mediated modulation of exopher formation, we investigated the *str-173* role in this pathway.

The wrmScarlet CRISPR/Cas9-mediated knock-in for the *str-173* gene confirmed its strong expression in ASK neurons and revealed additional expression in OLQ neurons, the pharynx, vulva muscles, and the tail (Extended Data Fig. 3a-b). Next, we created *str-173* null mutants again using CRISPR/Cas9 editing (Extended Data Fig. 3c) and observed that the basal level of exophergenesis was comparable to the wild-type control (Extended Data Fig. 3d). However, exophergenesis was lower for *str-173* null mutants grown as a single animal on their own plate compared to the wild-type control (Extended Data Fig. 3e). Moreover, *str-173* mutants exhibit a smaller increase in exopher production in response to male pheromones (Extended Data Fig. 3f). This finding suggests that STR-173 plays a role in the signal processing that occurs in response to the metabolites secreted by other worms.

Among the 118 classes of neurons in *C. elegans*, only four are directly exposed to the pseudocoelomic cavity[38]. Three classes of these neurons, AQR, PQR, and URX regulate social feeding in worms[39]. Given that exophers are released to the worm's pseudocoelomic cavity and are regulated by social cues, we hypothesized that AQR, PQR, and URX might play a role in exophergenesis regulation. To test for that, we first investigated the effect of genetic ablation of AQR, PQR, and URX neurons on exopher production. Indeed, the removal of these neurons leads to a substantial increase in exophergenesis (Fig. 4a). Notably, the increased number of

exophers generated by worms with genetically ablated AQR, PQR, and URX neurons is not the result of embryo-maternal signaling as these animals contain an even lower number of eggs *in utero* (Fig. 4b) and have a smaller brood size (Extended Data Fig. 4a-b) than wild-type control.

To further validate the role of AQR, PQR, and URX neurons in the regulation of exophergenesis, we optogenetically inactivated or activated them using ArchT[40] or ReaChR[41], respectively, and compared the number of exophers before and after the stimulus. We observed that 60 min of AQR, PQR, and URX neuron inactivation leads to a significant increase in exopher release (Fig. 4c and Extended Data Fig. 4c). On the other hand, 60 min of AQR, PQR, and URX neuron activation resulted in a significant decrease in exopher release after the stimulus was completed (Fig. 4d and Extended Data Fig. 4d).

Our data also demonstrates that opposing exophergenesis phenotypes in ASK-ablated animals and in worms with the genetic elimination of AQR, PQR, and URX are counterbalanced in worms with all four neuron classes removed (Fig. 4e). Finally, we show that AQR, PQR and URX participate in mediating response to hermaphrodite pheromones (Fig. 4f) but not to male pheromones (Fig. 4g) and their high activity is not sufficient to overcome the critical role of embryo-maternal signaling in exopher production (Fig. 4h-i). Altogether our data indicate that the volatile signals lowering exopher levels secreted by hermaphrodites act through the olfactory system and partly via AQR, PQR, and URX neurons. The male secretions detected by olfactory neurons, in turn, potentiate exophergenesis by promoting embryo accumulation *in utero*, and this triggers pro-exopher signals independent of the activity of AQR, PQR, and URX neurons (Fig. 4j).

Discussion

Sensory neurons, through various types of metabolites, tune the functionality of somatic tissues to environmental conditions. We demonstrated that this also applies to the production of exopher vesicles by muscles. Our data show that, depending on the type of ascaroside pheromone, exophergenesis can be up- or down-regulated within the *C. elegans* hermaphrodite population. This communication system enables individuals to optimally utilize their muscle resources for reproductive purposes depending on the biological and environmental context. Accordingly, the higher level of exophers in hermaphrodites exposed to male metabolites or mated with males is consistent with the idea that male pheromones promote resource allocation to the germline[42], and exophers may contribute to oocyte/embryo quality. However, increasing exophergenesis accelerates the age-related deterioration in worm muscle function[8]. This is also in accordance with Aprison and Ruvinsky's observations that hermaphrodites hasten development and somatic aging in the presence of males[43]. As such, exophers probably act as biological executors and carriers of information in inter-animal communication. This is also consistent with observations that *Drosophila* males secrete extracellular vesicles that are important for mating behavior[44], and the exchange of information between male and female flies leads to increased EV release from sperm secretory cells, which promotes fertility[45]. Therefore, this bidirectional regulation of physiological processes related to EV-mediated communication between animals appears to be evolutionarily conserved. In this regard, sensory neurons exposed to the body cavity are also anticipated to play a role. We showed that *C. elegans* AQR, PQR, and URX neurons, which monitor the metabolic state of the animal, transmit neuroendocrine signals to downregulate exophergenesis. Interestingly, these neurons belong to the class of ciliated neurons and their counterparts exposed to the environment are capable of extracellular vesicle production[6]. Therefore, it is tempting to speculate that AQR,

PQR, and URX could transmit biological information within the worm body using extracellular vesicles released to the pseudocoelomic cavity, which could assist classical neurotransmitters or neuropeptides. However, additional research is required to establish how this class of ciliated neurons suppresses exophers formation/release by BWM.

Using *C. elegans* as a model, we showed that exopher production in one tissue is controlled by signals from another. Similar programs that enable fine-tuning of cell-to-cell communication based on exophers facilitating efficient use of resources in multiple tissues may work in humans, as confirmed by studies on other classes of EVs[46]. Moreover, our results demonstrate the worm's olfactory system's importance in regulating exopher formation in muscles. Notably, olfactory dysfunction in humans has been shown to lead to an increased likelihood of cardiovascular disease (CVD)[47,48]. This could result from faulty regulation of exophergenesis in the heart, which helps maintain homeostasis during cardiac stress. However, additional research is required to determine whether mammals possess a comparable exopher control system depending on the olfactory network.

Figures and figure legends

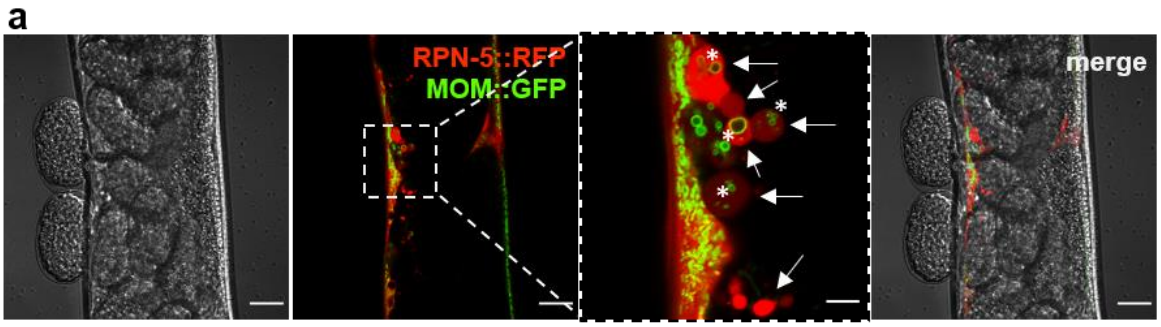

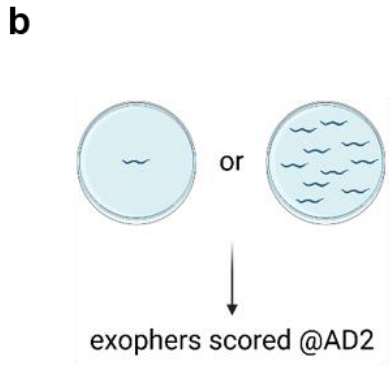

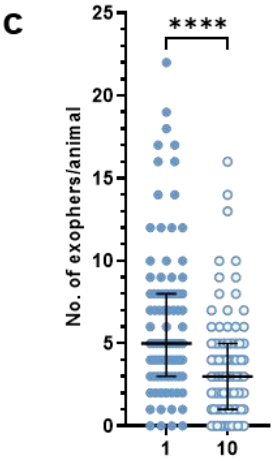

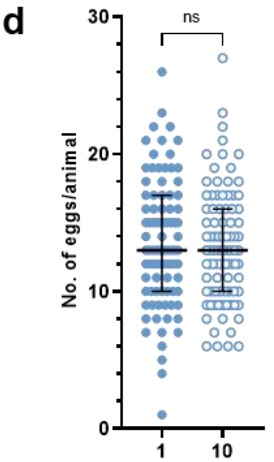

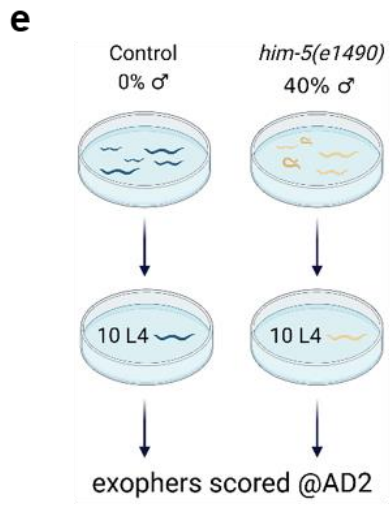

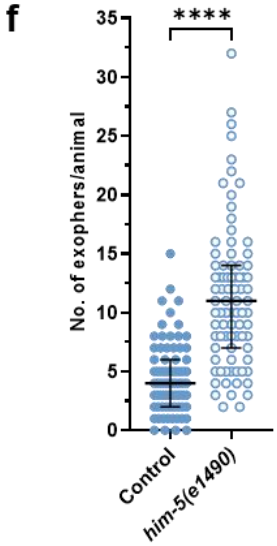

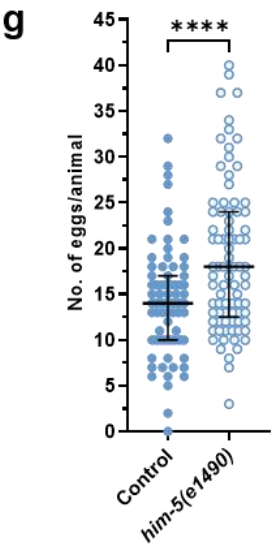

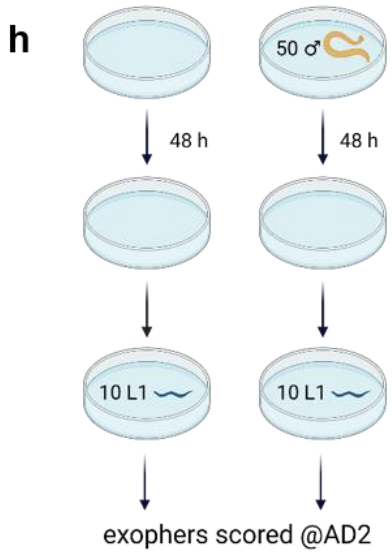

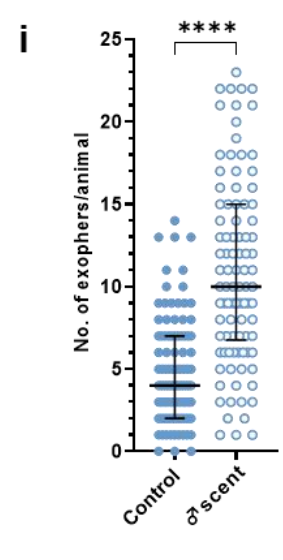

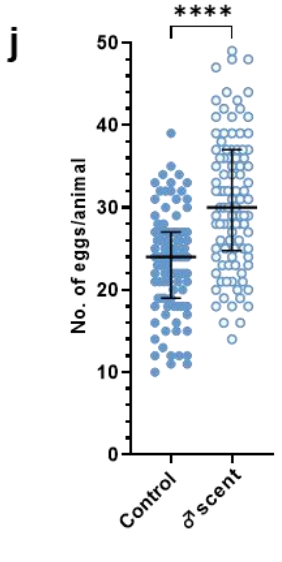

Figure 1. Production of *Caenorhabditis elegans* muscle exophers is regulated by hermaphrodites' and males' presence.

a An example of *C. elegans* muscle exopher containing mitochondria. Red fluorescence comes from RPN-5 proteasome subunit tagged with wrmScarlet fluorescent protein. Green fluorescence show mitochondrial outer membrane (MOM) tagged with GFP. Arrows point to examples of exophers, asterisks indicate mitochondria-containing exophers.

b Experimental design for determining the effect of the presence of other hermaphrodites on the number of exophers in a reporter strain.

c *C. elegans* hermaphrodites grown in the presence of other hermaphrodites produce fewer exophers than solitary animals. n = 88 and 90; N = 3.

d Embryo-maternal signaling is not responsible for the differences in exophergenesis levels as both solitary and accompanied hermaphrodites contain the same number of embryos *in utero*. n = 88 and 90; N = 3.

e Schematic representation of the experimental setup for investigating the influence of increased male presence in the population.

f Increased percentage of males in the population (via *him-5(e1490)* mutation) leads to a higher exophergenesis level in hermaphrodites. n = 79 and 83; N = 3

g Increased percentage of males in the population (via *him-5(e1490)* mutation) causes embryo retention in hermaphrodites. n = 79 and 85; N = 3

h Schematic representation of the experimental setup for investigating the influence of male's secretome on exophergenesis level.

i Growing hermaphrodites on male-conditioned plates increases exophergenesis levels. n = 106 and 98; N = 3.

j Exposing hermaphrodites to male secretome causes embryo retention in the uterus. n = 105 and 98; N = 3.

Data information: Scale bars are 20 μm and 5 μm (zoom in). @AD2 means “at adulthood day 2”. Data are presented as median with interquartile range; n represents the number of worms; N represents a number of experimental repeats that were combined into a single value; ns - not significant ($P > 0.1$), **** $P < 0.0001$; Mann-Whitney test.

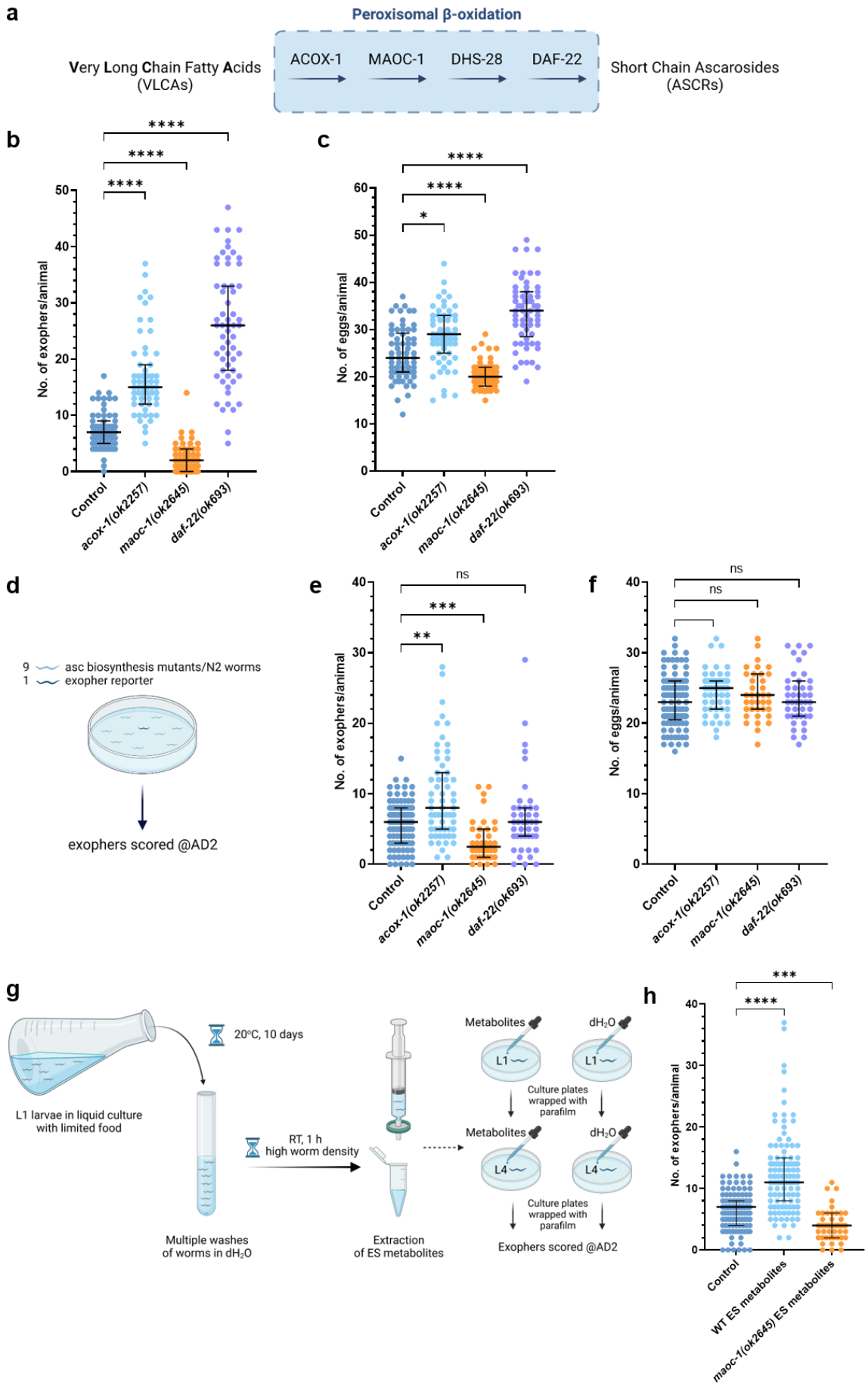

Figure 2. Ascaroside pheromones regulate muscle exopher production.

a Ascaroside side-chain biosynthesis.

b Ascaroside side-chain biosynthesis mutants produce various numbers of exophers. n = 59 - 66; N = 3.

c Mutation in genes encoding ascaroside side-chain biosynthesis enzymes influence *in utero* embryo presence. n = 59 - 66; N = 3.

d Schematic representation of the experimental setup for investigating the influence of ascaroside side-chain biosynthesis mutants presence on exophergenesis level in wild-type worms.

e Growing wild-type hermaphrodites in the presence of *acox-1(ok2257)* and *maoc-1(ok2645)* mutant increase and decrease exopher production, respectively. n = 38 - 93; N = 3.

f Growing wild-type hermaphrodites with ascaroside side-chain biosynthesis mutants does not influence the number of embryos present in the uterus. n = 37 - 93; N = 3.

g Schematic overview of the procedure for the isolation of metabolites from starving worms.

h Exposing worms to metabolites isolated from wild-type and *maoc-1(ok2645)* mutant starving populations oppositely regulate exopher production. n = 107 - 110, and 47 for *maoc-1(ok2645)*; N = 3 and N = 2 for *maoc-1(ok2645)*.

Data information: @AD2 means “at adulthood day 2”. Data are presented as median with interquartile range; n represents the number of worms; N represents a number of experimental repeats that were combined into a single value; ns - not significant ($P > 0.1$), * $P < 0.05$, ** $P < 0.01$, *** $P < 0.001$, **** $P < 0.0001$; Kruskal-Wallis test with Dunn's multiple comparisons test.

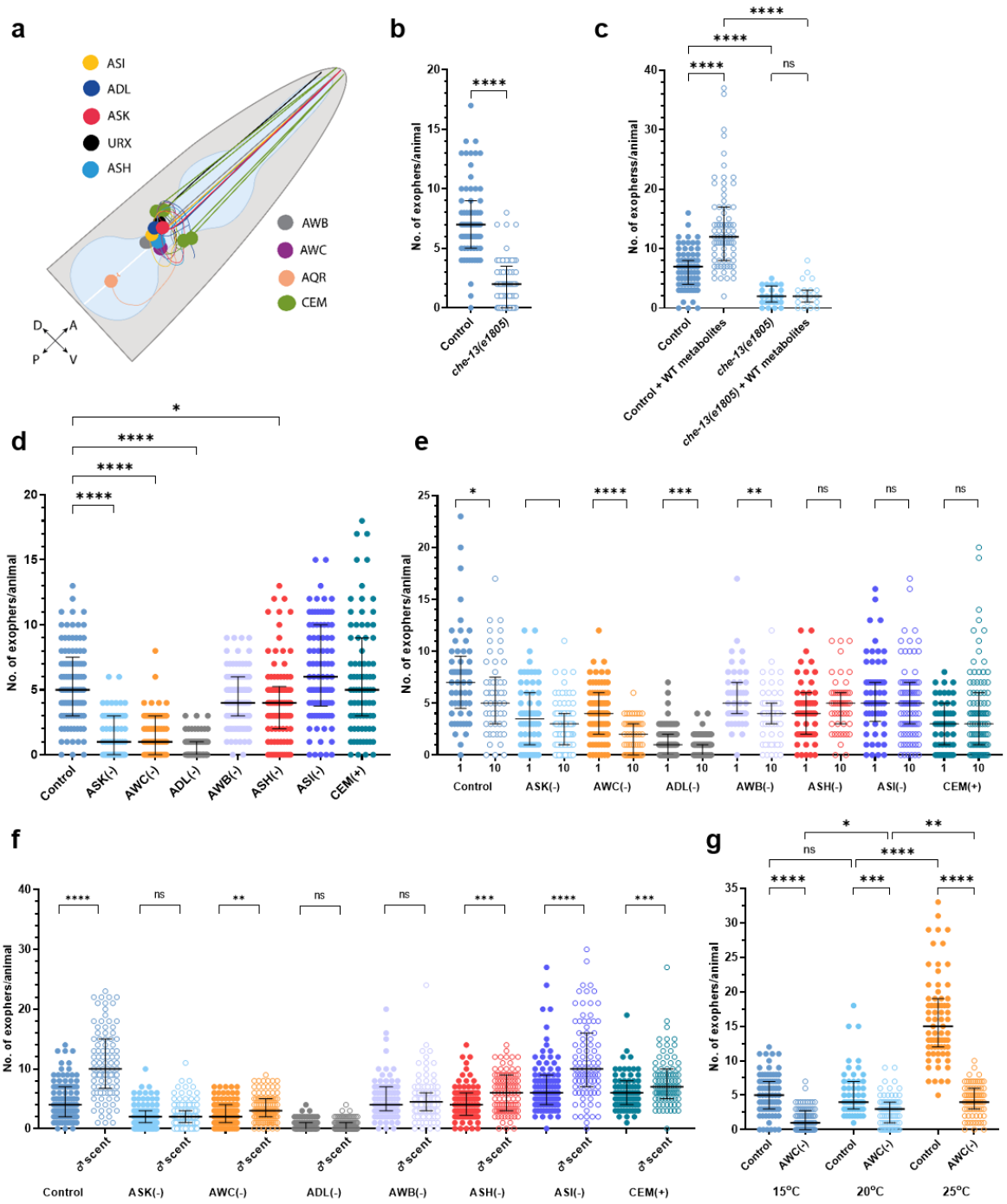

Figure 3. Multiple olfactory neurons regulate exophergenesis levels in response to hermaphrodite and male pheromones.

a Sensory neurons investigated within this study.

b Hermaphrodites with impaired ciliated sensory neurons have lower exophergenesis levels. n = 66 and 65; N = 3.

c Hermaphrodites with impaired ciliated sensory neurons do not produce more exophers in response to metabolites isolated from wild-type worms. n = 79 for Control and n = 19 - 24 for *che-13(e1805)*; N = 3 and 1, respectively.

d Genetic ablation of ASK, AWC, ADL, or ASH neurons reduces exopher production. n = 62 - 97; N = 3.

e Decrease in exophergenesis level due to exposure to hermaphrodite's pheromones is mediated by ASH, ASI, and ASK neurons, and can be altered by the addition of CEM male-specific neurons. n = 49 - 97; N = 3.

f Increase in exophergenesis levels due to exposure to male's pheromones is mediated by ASK, AWB, and ADL neurons. n = 77 - 108; N = 3.

g AWC neurons regulate the temperature-dependent increase in muscle exopher production. n = 52 - 92; N = 3.

Data information: Data are presented as median with interquartile range; n represents the number of worms; N represents a number of experimental repeats that were combined into a single value; ns - not significant ($P > 0.1$), * $P < 0.05$, ** $P < 0.01$, *** $P < 0.001$, **** $P < 0.0001$; (b, e, f) Mann-Whitney test, (c, d, g) Kruskal-Wallis test with Dunn's multiple comparisons test.

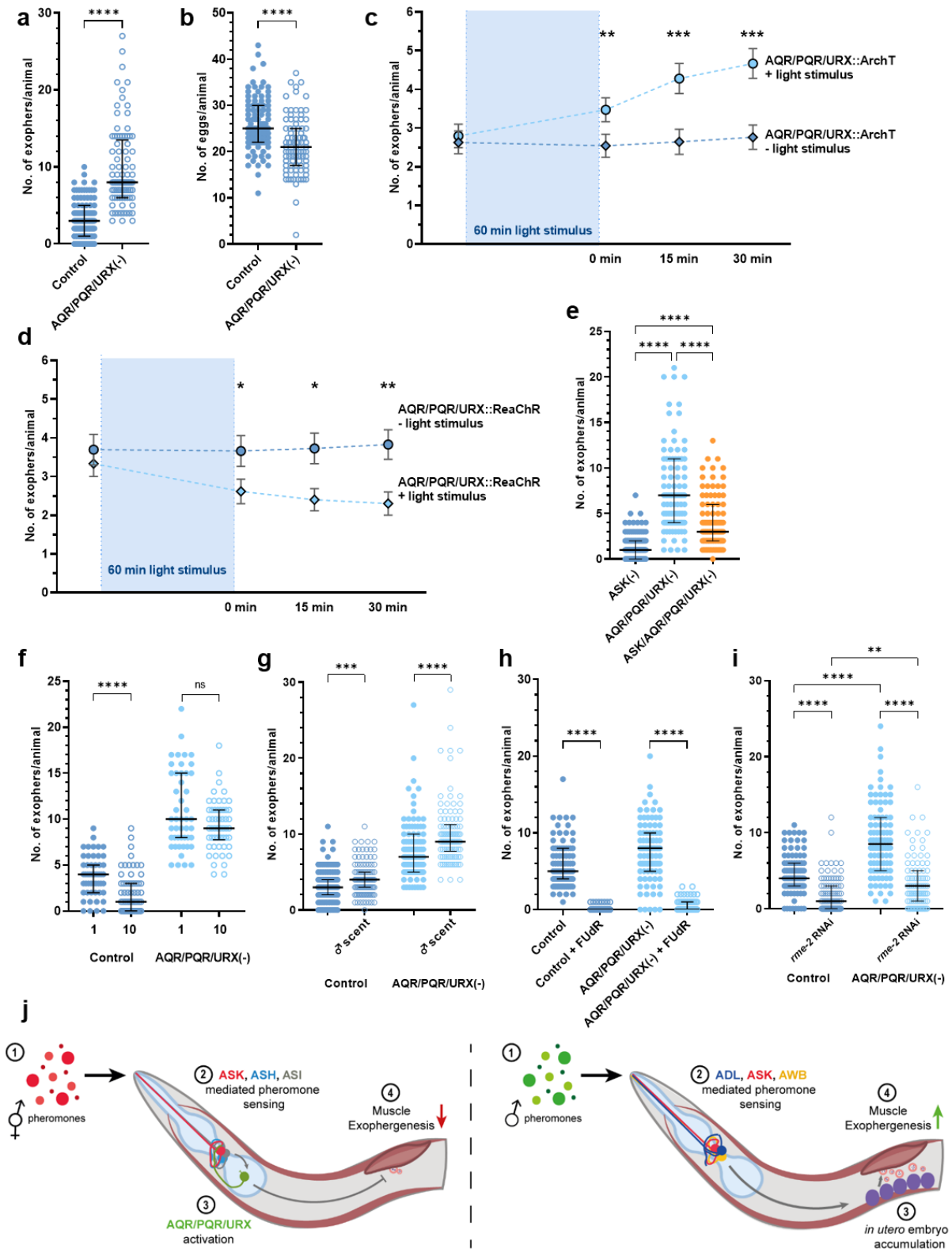

Figure 4. Pseudocoelom-exposed neurons negatively regulate exopher production.

a Genetic ablation of pseudocoelom-exposed AQR, PQR, and URX neurons increases exopher production. n = 89 and 100; N = 3.

b Genetic ablation of pseudocoelom-exposed AQR, PQR, and URX neurons causes a decrease in the number of embryos present in the uterus. n = 89 and 100; N = 3.

c ArchT-mediated optogenetic inactivation of AQR, PQR, and URX neurons leads to an increase in exopher production. n = 59; N = 6.

d ReaChR-mediated optogenetic activation of AQR, PQR, and URX neurons leads to a decrease in exopher production. n = 59 and 60; N = 6.

e Low exophergenesis level in animals with genetic ablation of ASK neurons and high level of exophergenesis in animals with genetic ablation of AQR, PQR, and URX neurons are equalized in animals with all four neurons removed. n = 90 - 106; N = 3.

f Decrease in exophergenesis level due to exposure to hermaphrodite's pheromones is partially mediated by AQR, PQR, and/or URX neurons. n = 51 - 60; N = 3.

g Increase in exophergenesis levels due to exposure to male pheromones is not altered in animals with genetic ablation of AQR, PQR, and URX neurons. n = 102 - 105; N = 3.

h Genetic ablation of AQR, PQR, and URX neurons do not rescue the inhibition of exophergenesis caused by FUdR-mediated worm sterility. n = 89 - 90; N = 3.

i Genetic ablation of AQR, PQR, and URX neurons only partially rescues the inhibition of exophergenesis caused by *rme-2* (yolk receptor) knockdown. n = 90; N = 3.

j Model for olfaction-dependent regulation of muscle extracellular vesicles formation. ASK, ASH, and ASI neurons sense hermaphrodite pheromones which leads to muscle exophergenesis down-regulation through AQR/PQR/URX activation. ASK, AWB, and ADL sense male pheromones which leads to muscle exophergenesis up-regulation through signaling derived from *in utero* accumulating embryos.

Data information: Scale bars are 20 μm. Data are presented as median with interquartile range; n represents the number of worms; N represents a number of experimental repeats that were combined into a single value; ns - not significant ($P > 0.1$), * $P < 0.05$, ** $P < 0.01$,*** $P <$

368 0.001, **** P < 0.0001; (a, c, d, e, g, h, i) Mann-Whitney test, (f, j) Kruskal-Wallis test with

369 Dunn's multiple comparisons test.

370

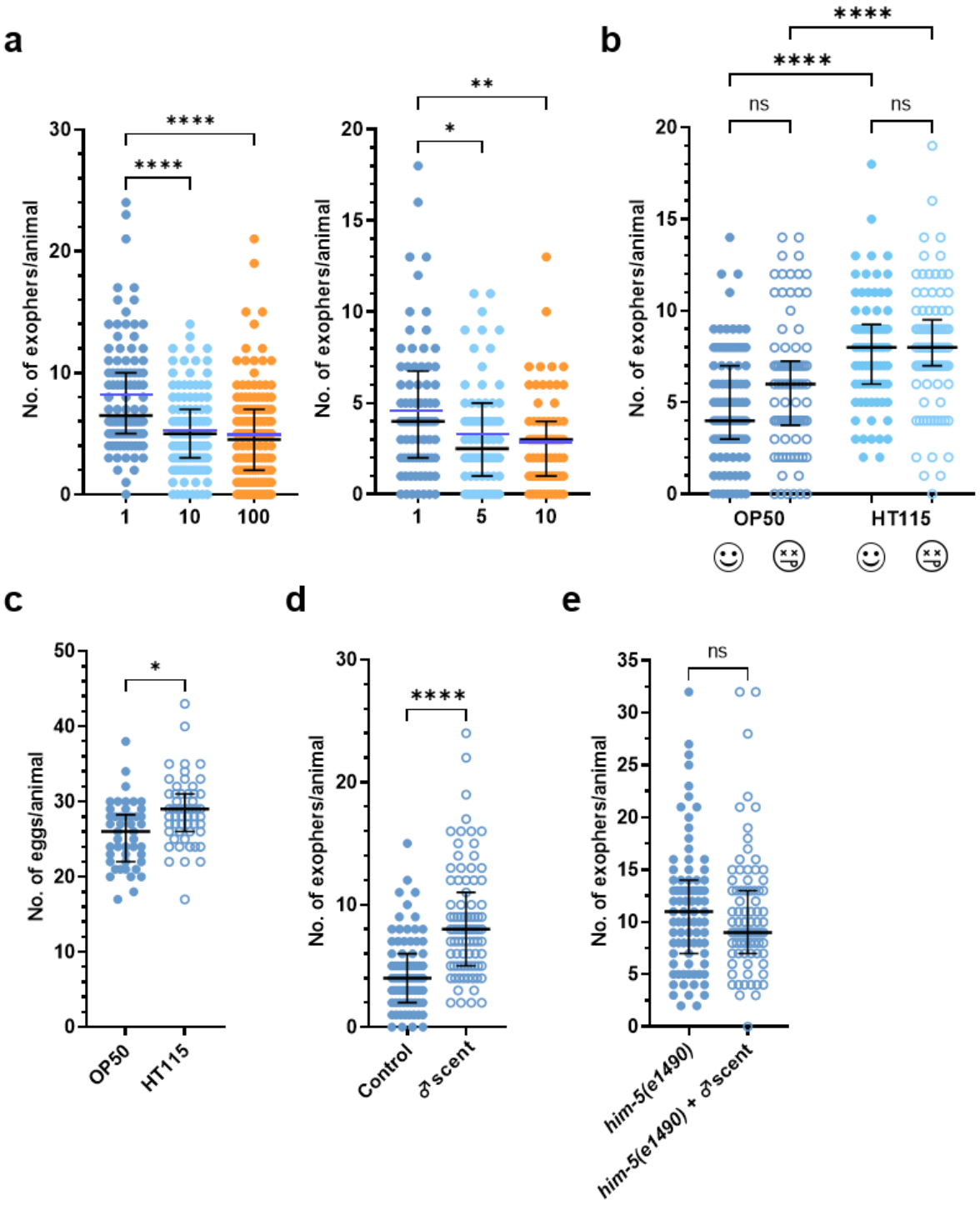

371

372 **Extended Data Figure 1. Influence of worm population composition and bacteria diet on**

373 **muscle exophers formation.**

a Exopher production is regulated by hermaphrodite-derived metabolites in a dose-dependent manner. n = 100 - 124 and n= 70 - 76; N = 3.

b Worms fed with metabolically active and inactive bacteria produce a similar number of exophers. Worms grown on *E. coli* HT115 strain produce more exophers than worms grown on *E. coli* OP50 strain. n = 78 - 93; N = 3.

c Worms grown on *E. coli* HT115 strain contain more eggs *in utero* than worms grown on *E. coli* OP50 strain. n = 46 and 55; N = 3.

d Growing hermaphrodites on male-conditioned plates increases exophergenesis levels regardless of *E. coli* strain used as a food source (HT115 – Fig.1i, OP50 – Extended Data Fig. 1d). n = 79 and 87; N = 3.

e Exposing hermaphrodites to a male's secretome above the L4 stage does not further increase exopher production. n = 83; N = 3.

Data information: Data are presented as median with interquartile range; violet bars represent mean value; n represents the number of worms; N represents a number of experimental repeats that were combined into a single value; ns - not significant ($P > 0.1$), * $P < 0.05$, ** $P < 0.01$, **** $P < 0.0001$; (c, d, e) Mann-Whitney test, (a, b) Kruskal-Wallis test with Dunn's multiple comparisons test.

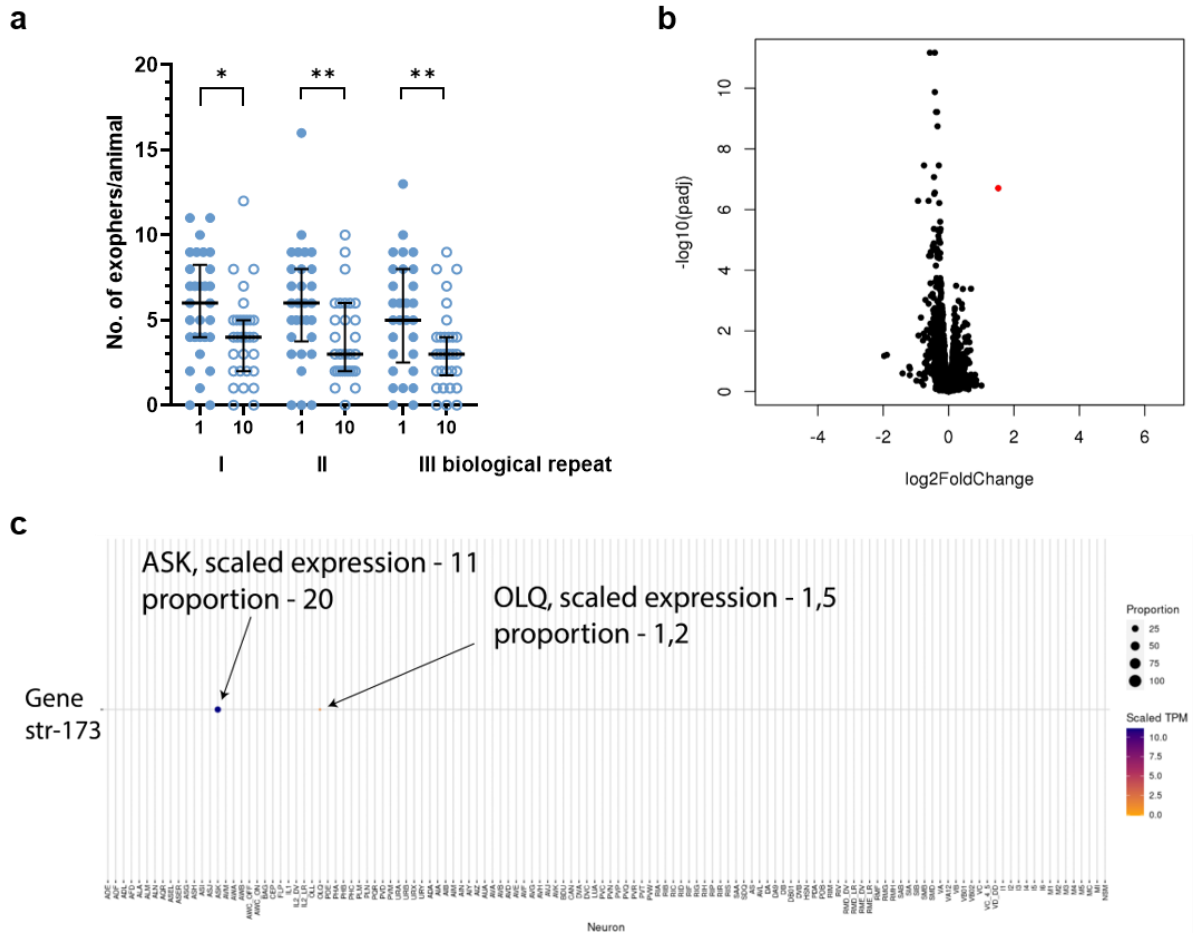

Extended Data Figure 2. Worms grown in populations with different densities did not differ significantly on the transcriptional level.

a Number of exophers produced by worms that were used for RNAseq analysis. n = 29 - 30; N = 3.

b Worms grown either as a single animal or in a ten-hermaphrodites population did not differ significantly on the transcriptional level. Transcript with significant change is marked as a red dot.

c Single-cell RNA-seq data from CeNGENApp[37] show *str-173* strong expression in ASK neurons and weak expression in OLQ neurons. Circle diameter represents the proportion of neurons in each cluster that express *str-173* gene.

403 Data information: Data are presented as median with interquartile range; n represents the
404 number of worms; N represents a number of experimental repeats that were combined into a
405 single value; * $P < 0.05$, ** $P < 0.01$; (**a**) Mann-Whitney test,

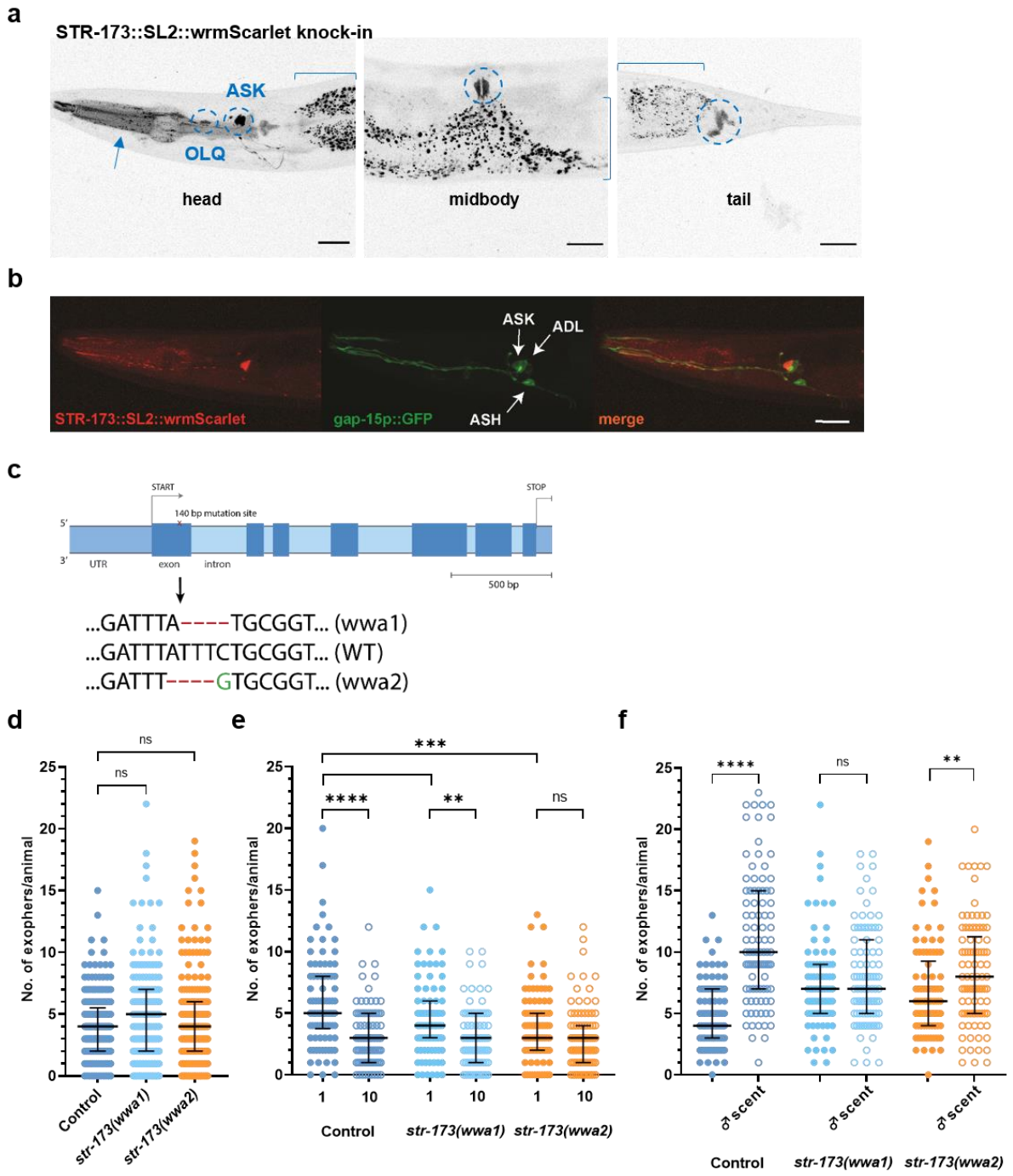

406

407 **Extended Data Figure 3. STR-173 receptor mediates pheromone-dependent**

408 **exophergenesis modulation**

409 **a - b** *str-173* 7TM receptor is expressed in neurons (ASK and OLQ(?)) and non-neuronal

410 tissues (pharynx marked with an arrow, vulva, and rectal gland(?) marked with circles). Square

411 brackets mark gut autofluorescence.

412 **c** Localization of *str-173* mutations in the gene.

d Basal level of exophergenesis in *str-173* mutants is unchanged compared to wild-type worms. n = 190 - 208; N = 6.

e Solitary *str-173* mutants produce a smaller number of exophers compared to wild-type worms. n = 90; N = 3.

f Increase in exophergenesis levels due to exposure to male pheromones is partially dependent on STR-173 7TM receptor. n = 89 - 94; N = 3.

Data information: Scale bars are (a) 30 μm and (b) 20 μm. Data are presented as median with interquartile range; n represents the number of worms; N represents a number of experimental repeats that were combined into a single value; ns - not significant ($P > 0.1$), ** $P < 0.01$, *** $P < 0.001$, **** $P < 0.0001$; (d, e) Kruskal-Wallis test with Dunn's multiple comparisons test, (f) Mann-Whitney test.

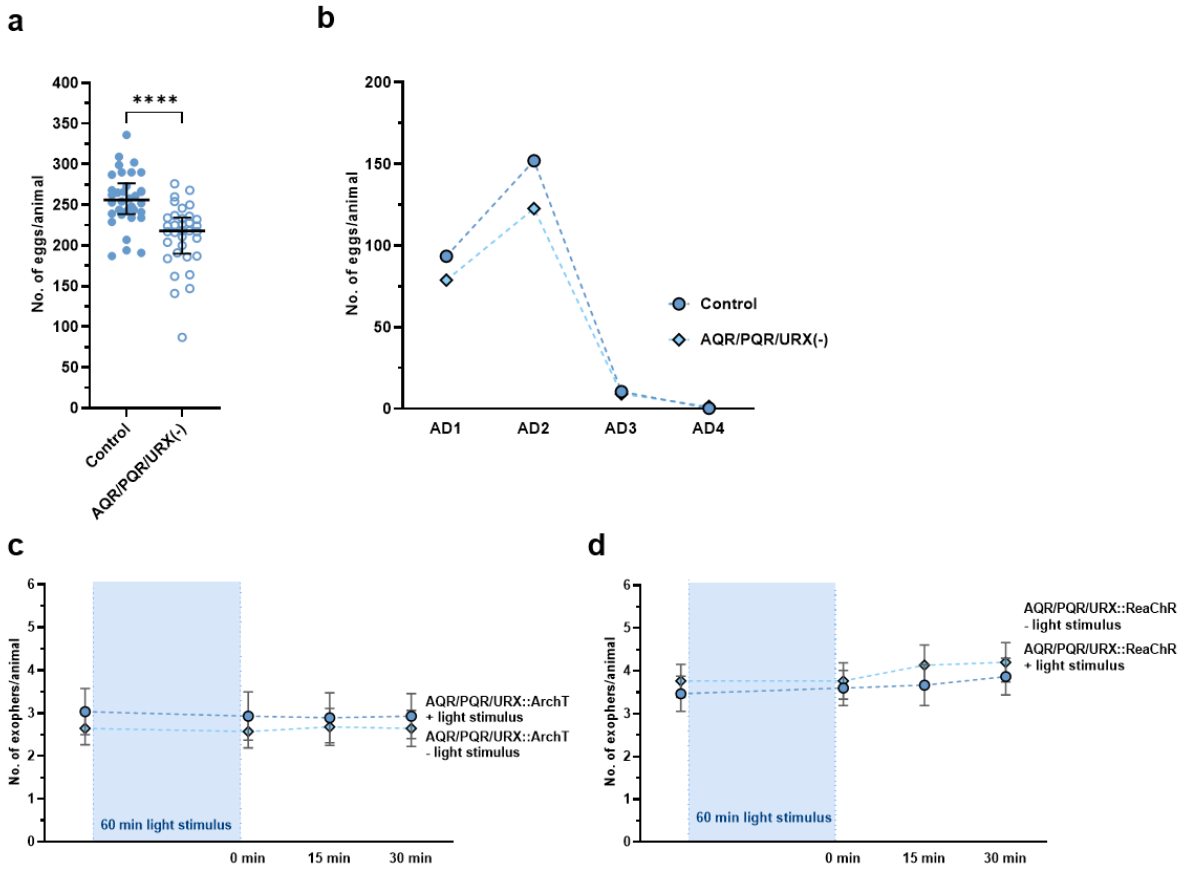

Extended Data Figure 4. Worms lacking AQR, PQR, and URX neurons have lower brood size than the wild type.

a - b Worms with the genetic ablation of pseudocoelom-exposed AQR, PQR, and URX neurons have lower brood size than the wild type. n = 34; N = 3.

c Control experiment without all-trans retinal (ATR) for ArchT-mediated inactivation of AQR, PQR, and URX neurons. n = 30; N = 3.

d Control experiment without all-trans retinal (ATR) for ReaChR-mediated activation of AQR, PQR, and URX neurons. n = 30; N = 3.

Data information: Data are presented as median with interquartile range; n represents the number of worms; N represents a number of experimental repeats that were combined into a single value; ns - not significant ($P > 0.1$), **** $P < 0.0001$; Mann-Whitney test.

439 **Supplementary Table 1.**

Gene.name	log2FoldChange	pvalue	padj
srw-86	2,470005259	0,006089231	NA
str-173	**1,210254202**	**0,083872612**	**NA**
sri-39	0,961870706	0,118312493	NA
srm-1	0,74631012	0,197705915	NA
srh-269	0,715357507	0,20128121	NA
sri-36	0,697436016	0,069365061	NA
str-55	0,69275127	0,286227955	NA
srd-64	0,671778641	0,227938718	NA
srsx-36	0,632246484	0,436691291	NA
sri-57	0,609273781	0,193809518	NA
srw-89	0,578848267	0,407242411	NA
srbc-82	0,56597091	0,423856002	NA
srr-2	0,523068614	0,103943944	NA
srx-97	0,505797282	0,424229255	NA
sri-11	0,489747472	0,297473585	NA
srv-15	0,463355568	0,372243301	NA
srj-14	0,460503239	0,065003699	NA
sre-36	0,458443613	0,346744567	NA
srh-217	0,429350684	0,444951979	NA
srh-2	0,409544299	0,241263936	NA
srx-41	0,39088958	0,531069383	NA
srr-10	0,382508507	0,600239609	NA
srz-97	0,370702424	0,498470233	NA
srsx-19	0,353102397	0,54270153	NA

srd-70	0,320458039	0,541451057	NA
srh-71	0,308999771	0,434944825	NA
str-179	0,291901118	0,596460956	NA
str-148	0,267146531	0,651806161	NA
sra-35	0,258242663	0,576292957	NA
srx-45	0,226491874	0,636877507	NA
srsx-27	0,225810039	0,724940673	NA
srr-6	0,223992203	0,491120033	NA
srb-16	0,213930895	0,686266407	NA
sri-55	0,204504014	0,648957813	NA
srx-125	0,196087663	0,632165424	NA
srw-48	0,1760458	0,784611201	NA
sri-35	0,174186697	0,816308334	NA
srsx-25	0,172603337	0,699023544	NA
srj-29	0,145173827	0,82575966	NA
str-176	0,145080793	0,381737839	0,705706926
srv-32	0,140744356	0,836820773	NA
srj-52	0,12758145	0,8360209	NA
srab-4	0,123433522	0,75301419	NA
srxa-14	0,122166676	0,825629763	NA
src-1	0,121226527	0,017785109	0,153059765
srr-4	0,118248088	0,143496801	0,45832863
srsx-34	0,118146738	0,517657949	NA
str-144	0,115566741	0,882522042	NA
sri-8	0,114856655	0,747072742	NA
srh-48	0,107505544	0,732564142	NA
str-245	0,085385814	0,731316789	NA

srv-7	0,081868619	0,676931931	NA
srj-9	0,057842686	0,909552581	NA
sra-33	0,04490344	0,924342693	NA
srsx-18	0,037063376	0,9551973	NA
src-2	0,006822308	0,971252278	NA
srr-1	0,00459541	0,99125387	NA
sri-59	0,000405882	0,999217048	NA
srg-34	-0,030080578	0,947775572	NA
str-172	-0,085472421	0,87286706	NA
srr-3	-0,088516378	0,76868265	NA
srd-32	-0,107551827	0,816267341	NA
srv-1	-0,11334895	0,410156047	0,727497177
srh-237	-0,151085831	0,175026351	0,503664735
str-183	-0,178110179	0,787945578	NA
sra-10	-0,178642194	0,779315606	NA
sra-32	-0,190091468	0,685526539	NA
srd-14	-0,207486411	0,305360875	NA
sre-13	-0,210537797	0,702655411	NA
srd-52	-0,235477439	0,677464298	NA
sri-40	-0,247157736	0,037111528	0,232197335
srz-85	-0,247831631	0,640803343	NA
sra-14	-0,266593158	0,200655026	NA
srh-16	-0,275054658	0,57204149	NA
srh-70	-0,322126344	0,575669232	NA
srab-14	-0,328373116	0,605637275	NA
srx-12	-0,361291214	0,429781376	NA
sre-9	-0,397855081	0,275566108	NA

srx-58	-0,458521562	0,487282023	NA
sri-5	-0,458897325	0,308597251	NA
srt-23	-0,460153207	0,606235802	NA
srm-3	-0,470085367	0,174616055	NA
srh-33	-0,479357546	0,48607886	NA
srh-105	-0,486191119	0,439431381	NA
srw-35	-0,492290252	0,480189518	NA
srx-118	-0,521178132	0,380103143	NA
srm-5	-0,557246057	0,448970879	NA
srd-53	-0,588697815	0,325322641	NA
str-168	-0,611511779	0,293797037	NA
sre-4	-0,659337898	0,279814818	NA
srx-98	-0,789769153	0,126804165	NA
srt-39	-0,803397597	0,204138417	NA
srz-99	-0,866876045	0,048915705	NA
sre-44	-1,105518367	0,091985454	NA

440

441 **Materials and Methods**

442 **Reagents and Tools table**

Reagent or Resource	Source	Identifier
Bacterial and Virus Strains		
Escherichia coli RNAi feeding strain	Caenorhabditis Genetics Center	HT115(DE3)
E. coli feeding strain	Caenorhabditis Genetics Center	OP50
Ahringer RNAi library	Source BioScience	*C. elegans* RNAi Collection (Ahringer)
Chemicals, Peptides, and Recombinant Proteins		
All-trans retinal	Sigma-Aldrich	R2500
Bacto Agar	BioShop	AGR001.1

Bacto Peptone	BioShop	PEP403.1
Bacto Tryptone	BioShop	TRP402.1
Sodium Chloride	Chempur	117941206
Streptomycin sulfate salt	Sigma-Aldrich	S6501
Nystatin suspension 10,000 unit/mL	Sigma-Aldrich	N1638
Carbenicillin disodium salt	Roth	6344.2
Magnesium Sulfate heptahydrate	Sigma-Aldrich	M5921
Potassium dihydrogen phosphate	Roth	3904.1

di-potassium hydrogen phosphate	Roth	P749.1
Calcium Chloride (dihydrate)	BioShop	CCL444.500
Cholesterol	BioShop	CHL500.5
Tetracycline HCl	BioShop	TET701
IPTG	BioShop	IPT001
Polystyrene microspheres	Polysciences Europe GmbH	08691-10
Tetramisole hydrochloride	Sigma-Aldrich	L9756
Paraformaldehyde	Sigma-Aldrich	158127

5-Fluoro-2'-deoxyuridine	Sigma-Aldrich	F0503	
Sodium hypochlorite solution 14%	VWR	27900	
***Caenorhabditis elegans* strains**			
Genotype	**Source**	**Identifier**	**Description**
wacIs1[myo-3p::rpn-5 CAI = 0.97::GGGGS Linker-wrmScarlet::unc-54 3′UTR, unc-119(+)]	This paper	Strain ACH81	Strain with muscle exopher RFP marker in N2 wild-type background
wacIs1[myo-3p::rpn-5 CAI = 0.97::GGGGS Linker-wrmScarlet::unc-54 3′UTR, unc-119(+)],	Turek *et al.*, 2021	Strain ACH93	Strain with muscle exopher RFP and mitochondrial

wacIs14[myo-3 promoter::tomm-20_1–50aa::attB5::mGFP::unc-54-3′UTR, unc-119(+)]			GFP marker in N2 wild-type background
daf-22(ok693)	CGC	Strain RB859	
wacIs1[myo-3p::rpn-5 CAI = 0.97::GGGGS Linker-wrmScarlet::unc-54 3′UTR, unc-119(+)], wacIs14[myo-3 promoter::tomm-20_1–50aa::attB5::mGFP::unc-54-3′UTR, unc-119(+)]; daf-22(ok693)	This paper	Strain WOP456	Strain with muscle exopher RFP and mitochondrial GFP marker in *daf-22(ok693)* mutant background
acox-1(ok2257)	CGC	Strain VC1785	

wacIs1[myo-3 promoter::rpn-5 CAI=0.97::GGGGS Linker-wrmScarlet::unc-54 3'UTR, unc-119(+)], wacIs14[myo-3 promoter::tomm-20_1-50aa::attB5::mGFP::unc-54-3'UTR, unc-119(+)]; acox-1(ok2257) I	This paper	Strain TUR7	Strain with muscle exopher RFP and mitochondrial GFP marker in *acox-1(ok2257)* mutant background
maoc-1&E04F6.6(ok2645) II.	CGC	Strain RB2000	
wacIs1[myo-3 promoter::rpn-5 CAI=0.97::GGGGS Linker-wrmScarlet::unc-54 3'UTR, unc-119(+)]; maoc-1&E04F6.6(ok2645) II	This paper	Strain TUR46	Strain with muscle exopher RFP marker in *maoc-1&E04F6.6(ok2645)* mutant background

wacIs1[myo-3 promoter::rpn-5 CAI=0.97::GGGGS Linker-wrmScarlet::unc-54 3'UTR, unc-119(+)], wacIs14[myo-3 promoter::tomm-20_1-50aa::attB5::mGFP::unc-54-3'UTR, unc-119(+)]; che-13(e1805)	This paper	Strain TUR11	Strain with muscle exopher RFP and mitochondrial GFP marker in *che-13(e1805)* mutant background
wacIs1[myo-3 promoter::rpn-5 CAI=0.97::GGGGS Linker-wrmScarlet::unc-54 3'UTR, unc-119(+)], wacIs14[myo-3 promoter::tomm-20_1-50aa::attB5::mGFP::unc-54-3'UTR, unc-119(+)]; qrIs2 [sra-9::mCasp1]	This paper	Strain TUR16	Strain with muscle exopher RFP, mitochondrial GFP marker, and ASK neuron genetic ablation

wacIs1[myo-3 promoter::rpn-5 CAI=0.97::GGGGS Linker-wrmScarlet::unc-54 3'UTR, unc-119(+)], wacIs14[myo-3 promoter::tomm-20_1-50aa::attB5::mGFP::unc-54-3'UTR, unc-119(+)]; hlh-4(tm604) III	This paper	Strain TUR75	Strain with muscle exopher RFP, mitochondrial GFP marker, and ADL neuron genetic ablation
wacIs1[myo-3 promoter::rpn-5 CAI=0.97::Optimal Linker-wrmScarlet::unc-54 3'UTR, unc-119(+)]; oyIs85 [ceh-36p::TU#813 + ceh-36p::TU#814 + srtx-1p::GFP + unc-122p::dsRed]	This paper	Strain WOP499	Strain with muscle exopher RFP, mitochondrial GFP marker, and AWC neuron genetic ablation

wacIs1[myo-3 promoter::rpn-5 CAI=0.97::GGGGS Linker-wrmScarlet::unc-54 3'UTR, unc-119(+)], wacIs14[myo-3 promoter::tomm-20_1-50aa::attB5::mGFP::unc-54-3'UTR, unc-119(+)]; oyIs84 [gpa-4p::TU#813 + gcy-27p::TU#814 + gcy-27p::GFP + unc-122p::DsRed]	This paper	Strain TUR49	Strain with muscle exopher RFP, mitochondrial GFP marker, and ASI neuron genetic ablation
wacIs1[myo-3 promoter::rpn-5 CAI=0.97::GGGGS Linker-wrmScarlet::unc-54 3'UTR, unc-119(+)], wacIs14[myo-3 promoter::tomm-20_1-50aa::attB5::mGFP::un	This paper	Strain TUR47	Strain with muscle exopher RFP, mitochondrial GFP marker, and ASH neuron genetic ablation

c-54-3'UTR, unc-119(+)]; peIs1713 [sra-6p::mCasp-1 + unc-122p::mCherry]			
wacIs1[myo-3 promoter::rpn-5 CAI=0.97::GGGGS Linker-wrmScarlet::unc-54 3'UTR, unc-119(+)], wacIs14[myo-3 promoter::tomm-20_1-50aa::attB5::mGFP::unc-54-3'UTR, unc-119(+)]; peIs1715 [str-1p::mCasp-1 + unc-122p::GFP]	This paper	Strain TUR51	Strain with muscle exopher RFP, mitochondrial GFP marker, and AWB neuron genetic ablation
wacIs1[myo-3 promoter::rpn-5 CAI=0.97::GGGGS Linker-wrmScarlet::unc-54 3'UTR, unc-119(+)],	This paper	Strain TUR18	Hermaphrodites of this strain have muscle exopher RFP, mitochondrial

wacIs14[myo-3 promoter::tomm-20_1-50aa::attB5::mGFP::unc-54-3'UTR, unc-119(+)]nIs133 [pkd-2::GFP] I, ceh-30(n3714) X			GFP marker, and contain CEM male-specific ciliated sensory neurons
wacIs1[myo-3 promoter::rpn-5 CAI=0.97::GGGGS Linker-wrmScarlet::unc-54 3'UTR, unc-119(+)], qaIs2241[gcy-36::egl-1 + gcy-35::GFP + lin-15(+)]	This paper	Strain TUR37	Strain with muscle exopher RFP marker and AQR/PQR/URX neurons genetic ablation
wacIs1[myo-3 promoter::rpn-5 CAI=0.97::GGGGS Linker-wrmScarlet::unc-54 3'UTR, unc-119(+)], wacIs14[myo-3	This paper	Strain TUR20	Strain with muscle exopher RFP and mitochondrial GFP marker in *str-173(wwa1)*

promoter::tomm-20_1-50aa::attB5::mGFP::unc-54-3'UTR, unc-119(+)]; str-173(wwa1) IV			mutant background
wacIs1[myo-3 promoter::rpn-5 CAI=0.97::GGGGS Linker-wrmScarlet::unc-54 3'UTR, unc-119(+)], wacIs14[myo-3 promoter::tomm-20_1-50aa::attB5::mGFP::unc-54-3'UTR, unc-119(+)]; str-173(wwa2) IV	This paper	Strain TUR21	Strain with muscle exopher RFP and mitochondrial GFP marker in *str-173(wwa2)* mutant background
wacIs1[myo-3 promoter::rpn-5 CAI=0.97::GGGGS Linker-wrmScarlet::unc-54 3'UTR, unc-119(+)],	This paper	Strain TUR59	Strain with muscle exopher RFP and mitochondrial GFP marker in

wacIs14[myo-3 promoter::tomm-20_1-50aa::attB5::mGFP::unc-54-3'UTR, unc-119(+)]; him-5(e1490) V			*him-5(e1490)* mutant background
wacIs1[myo-3 promoter::rpn-5 CAI=0.97::GGGGS Linker-wrmScarlet::unc-54 3'UTR, unc-119(+)]; wacIs14[myo-3 promoter::tomm-20_1-50aa::attB5::mGFP::unc-54-3'UTR, unc-119(+)]; wwaEx4[gcy-36 promoter::ReaChR::mKate2::unc-54 3'UTR, unc-119(+); myo-2 promoter::mNeonGreen]	This paper	Strain TUR38	Strain with muscle exopher RFP, mitochondrial GFP marker, and ReaChR for optogenetic activation of AQR, PQR, and URX

wacIs1[myo-3 promoter::rpn-5 CAI=0.97::GGGGS Linker-wrmScarlet::unc-54 3'UTR, unc-119(+)]; wacIs14[myo-3 promoter::tomm-20_1-50aa::attB5::mGFP::unc-54-3'UTR, unc-119(+)]; wwaEx9[gcy-36 promoter::ArchT::mKate2::unc-54 3'UTR, unc-119(+); myo-2 promoter::mNeonGreen]	This paper	Strain TUR43	Strain with muscle exopher RFP, mitochondrial GFP marker, and ArchT for optogenetic inactivation of AQR, PQR, and URX
str-173(syb6501[str-173::SL2-wrmScarlet]) IV	This paper	PHX6501	Endogenous translational reporter strain for *str-173* expression

str-173(syb6501[str-173::SL2-wrmScarlet]) IV, pkIs591[dpy-20(+) + gap-15::GFP]	This paper	TUR77	Endogenous translational reporter strain for *str-173* expression crossed with strain expressing GFP in ASK, ADL, ASH, PHA, an PHB
wacIs1[myo-3 promoter::rpn-5 CAI=0.97::GGGGS Linker-wrmScarlet::unc-54 3'UTR, unc-119(+)], wacIs14[myo-3 promoter::tomm-20_1-50aa::attB5::mGFP::unc-54-3'UTR, unc-119(+)]; qrIs2 [sra-9::mCasp1];	This paper	Strain TUR61	Strain with muscle exopher RFP, mitochondrial GFP marker, and ASK/AQR/PQR/URX neurons genetic ablation

qaIs2241[gcy-36::egl-1 + gcy-35::GFP + lin-15(+)]			
wacIs1[myo-3 promoter::rpn-5 CAI=0.97::GGGGS Linker-wrmScarlet::unc-54 3'UTR, unc-119(+)], wacIs14[myo-3 promoter::tomm-20_1-50aa::attB5::mGFP::unc-54-3'UTR, unc-119(+)]; qaIs2241[gcy-36::egl-1 + gcy-35::GFP + lin-15(+)]	This paper	Strain TUR62	Strain with muscle exopher RFP, mitochondrial GFP marker, and AQR/PQR/URX neurons genetic ablation
wild type	Caenorhabditis Genetics Center	Strain N2	*C. elegans* wild isolate
Recombinant DNA			

Plasmid: pGLOW77 (myo-2 promoter::mNeonGreen)	Addgene	#177338
Plasmid: pAS01 (gcy-36 promoter::ReaChR::mKate2-unc-54 3'UTR in pCG150)	This paper	N/A
Plasmid: pAS02 (gcy-36 promoter::ArchT::mKate2-unc-54 3'UTR in pCG150)	This paper	N/A
Plasmid: pAZ03 (mKate2-unc-54 3'UTR in pCG150)	This paper	N/A
Plasmid: ArchT (ArchT template)	gift from Bringmann Lab	N/A

Plasmid: ReaChR (ReaChR template)	gift from Bringmann Lab	N/A
Plasmid: mKate2-unc-54 3'UTR (mKate2-unc-54 3'UTR template)	gift from Bringmann Lab	N/A
Plasmid: pMH389 (gcy-36 promoter template)	gift from Kapitein Lab	N/A
Plasmid: pCG150	Addgene	#17247
Oligonucleotides		
Used for *acox-1(ok2257)* genotyping	FP1 AGTAGAGGC TGACGGGAC TT FP2 CTCGCTCGTT	RP GGGCAAATGGACATCAAGG C

	ACCTCGTCAA	
Used for *che-13(e1805)* genotyping	FP1 ATCCGTATTGCTTTGGAGAACGCTGTA FP2 GAGTTCATCTGTTCAAGATGAAGACGCC	RP1 TGATGAGTTTCAGAAGAATCCACGCC RP2 CAGTGGATGAGCAAGATGAAGATGATGA
Used for *daf-22(ok693)* genotyping	FP ACATTTGCCACGTAGCTGGT	RP1 TGGGCCGAGACAAAGCTTAC RP2 GTGGTAAGGGAAAAGCGCAA
Used for *maoc-1(ok2645)* genotyping	FP ACACGTTGT	RP1 AGTCTTGACCCCATGTGTTGA

	ACATCTCTCC CG	RP2 CAGCAATTGAACCACGTCCA
Used for creating pAS01		
-gcy-36	FP TATGACCAT GATTACGCC AAGCTATCT GGCACACTT TTTATTTCCA TAAACCTGC	RP TTGGCGCGCCCCACTTTGTA CAAGAAAGCTGGGTTCCGG ATCCTCCTCCGGATC
-ReaChR	FP AAATTCAAA CAAGGGCTA CCCAACAAT GGTCTCCCG TCGTCCATG	RP TTGGCGCGCCCCACTTTGTA CAAGAAAGCTGGGTTCCGG ATCCTCCTCCGGATC

Used for creating pAS02		
-gcy-36	FP TATGACCATGATTACGCCAAGCTATCTGGCACACTTTTTATTTCCATAAACCTGC	RP TTGGAGGGCGATTGGGTCCATTTTTTGTTGGGTAGCCCTTGTTTGAATTTAC
-ArchT	FP AAATTCAAACAAGGGCTACCCAACAAAAAATGGACCCAATCGCCCTC	RP TTGGCGCGCCCCACTTTGTACAAGAAAGCTGGGTTTTCCTCCTGGCTCTGGGG
Software and Algorithms		

GraphPad Prism 9	GraphPad Software, Inc.	N/A
ZEN	Zeiss	N/A
Office 365	Microsoft	N/A
ImageJ	Wayne Rasband (NIH)	N/A
BioRender	BioRender.com	N/A
Adobe Illustrator CS6	Adobe	N/A

Methods and Protocols

Worm maintenance and strains

Worms were maintained on nematode growth medium (NGM) plates seeded with bacteria *Escherichia coli* OP50 or HT115 at 20°C unless stated otherwise[17] A list of all *C. elegans* strains used in the study is provided in the table at the beginning of the "Materials and Methods" section.

Scoring exophers and fluorescence microscopy

For the assessment of exophers number, the protocol described in Turek *et al*. and Banasiak *et al*. (Bio-Protocol, detailed, step-by-step guide) was applied. Briefly, exophers were scored using stereomicroscope Zeiss Axio Zoom.V16 with filter sets 63 HE and 38 HE. For each exopher scoring assay, worms were age-synchronized from pretzel-stage embryos, L1 larvae, or L4 larvae. On adulthood day-2, animals were visualized on NGM plates, and the number of exophers was counted in each freely moving worm.

The representative pictures presented in the manuscript were acquired with an inverted Zeiss LSM800 laser-scanning confocal microscope with a 40x oil immersion objective. To excite the GFP and RFP fluorescent proteins, 488- and 561-nm lasers were used. For visualization, animals were immobilized on 3% agarose pads with 6µl of PolySciences 0.05 µm polystyrene microspheres or 25 µM tetramisole.

RNA interference assay

RNA interference in *C. elegans* was performed using the standard RNAi feeding method and RNAi clone[49], previously described in Turek *et al.*, 2021[8]. Briefly, NGM plates, supplemented with 12,5µg/ml tetracycline, 100µg/ml ampicillin and 1mM IPTG, were seeded with HT115 *E. coli* bacteria containing dsRNA against the gene of interest. Control group animals were fed with bacteria containing the empty vector. Age-synchronized pretzel-stage embryos or L1 larvae were placed on freshly prepared plates and cultured until day 2 of adulthood. The age of the worms was verified at the L4 larvae stage, either younger or older worms were removed from the experiment.

Pre-conditioning of the plates with *C. elegans* males

50 males from the strain with *him-5(e1490)* mutation were transferred on a fresh, 35 mm NGM plate with *E. coli* OP50 or HT115 at the L4 developmental stage and older. After 48 hours,

474 males were removed from the plates. L1 larvae were transferred to plates pre-conditioned with
475 males in a group of 10 animals per plate. For the control group, L1 larvae were transferred to
476 fresh, 35 mm NGM plates seeded with *E. coli* OP50 or HT115 without pre-conditioning with
477 males. Worms were cultured up to adulthood day 2 when muscle exophers were counted in
478 each animal.

479 **Egg retention assay**

480 Firstly, single worms were immobilized with 25 µM tetramizole on an NGM, bacteria-free
481 plate. Secondly, using the stereomicroscope, muscle exophers were counted in each worm. In
482 the following step, hermaphrodites were exposed to 1.8% hypochlorite solution. When they
483 dissolved, embryos retained in the uterus were counted.

484 **Metabolic inactivation of bacterial food source**

485 The preparation of plates with a metabolically inactive food source for the worms to determine
486 its effects on exophergenesis was done according to the protocol described in Beydoun *et al.*,
487 2021. Briefly, a single colony of *E. coli* HT115 or OP50 was inoculated overnight and then the
488 bacterial culture was split into two flasks. Next, paraformaldehyde (PFA) was added to a final
489 concentration of 0.5% in only one of them, and the flask was placed in the 37°C shaking
490 incubator for 1 h. Afterward, the aliquots were transferred to 50 mL tubes and centrifuged at
491 approximately 3000 × g for 20 min and washed with 25 mL of LB five times. Control and PFA-
492 treated bacteria were later concentrated accordingly and seeded on the NGM plates.

493 As control of PFA treatment, new bacterial cultures in LB were set in the 37°C shaking
494 incubator overnight to make sure the replication was blocked and there was no bacterial growth.

Plates were used for experiments at least 5 days after their preparation to make sure there are no bacteria-derived metabolites left on plates with PFA-treated *E. coli*. A new batch of bacterial food source was prepared for each biological repetition.

Brood size quantification

Age synchronized worms were transferred on fresh, 60mm NGM plates with *E. coli* OP50 or HT115 at the L4 developmental stage, single or two hermaphrodites on each of ten plates per biological repeat. Worms were transferred to fresh plates every day since adulthood day 1. The number of eggs laid over the worms' reproductive lifetime was counted manually every day. The data is presented as the total number of eggs laid by each animal or an average of the total number of eggs laid by each pair.

Quantifying number of exophers in worms grown in different temperatures

Worms were confronted with a range of physiological temperatures: low – 15^{o}C, optimal – 20^{o}C, and high – 25^{o}C throughout their development until exophers were scored. To compare the corresponding stages of development at various temperatures, worms were additionally sorted at the L4 stage. The exopher number was assessed based on the timepoint of maximal egg laying, approx. 140 h or 78 h from egg hatching at low or high temperatures of maintenance, respectively. Calculations of timing were based on the *C. elegans* development timeline at different temperatures[31].

Culturing worms in different population sizes

L1 larvae were transferred to 35 mm Petri dishes seeded with *E. coli* OP50 or HT115 bacteria strains (100 µL of bacteria from 10 mL overnight culture grown in 50 mL Erlenmeyer flask) immediately after hatching as a single larva or in a group of 5, 10 or 100 animals. In total, thirty

plates with single worms, six plates with 5 worms, three plates with 10 worms, and one plate with 100 worms were used per biological repeat.

Quantifying the influence of molecules released by ascaroside biosynthesis mutant on exopher production in wild-type worms

Nine freshly hatched L1 larvae from selected ascaroside biosynthesis mutant strains (*maoc-1(ok2645), daf-22(ok693),* or *acox-1(ok2257))* or wild-type hermaphrodites (as a control) were transferred to fresh NGM plates. Next, one L1 larva of a reporter strain expressing RFP in BWM was added to each plate and 10 worms in total were grown together.

Isolation of excretory-secretory (ES) metabolites containing ascarosides

Liquid-culture protocol for synchronous dauer formation from Cell Press STAR PROTOCOLS was applied step-by-step (Hibshman *et al*., 2020). Larvae enter dauer diapause by day 4-5 and dauers can be maintained for min. 40 days without a decrease in viability or the ability to recover. For the convenience of experimental conduct, wild-type and *maoc-1(ok2645)* larvae were maintained in liquid culture for 11 days before the isolation of excretory-secretory products.

On day 11 of liquid culture, worms were washed several times with S-medium to remove any possibly remaining debris and finally concentrated to approx. 30,000 dauers/mL. They were then rinsed three times with water and incubated for one hour on an orbital shaker at room temperature. After one hour they were centrifuged as described in Kaplan *et al.*[21] and the liquid with worm excretory-secretory products was filtered on ice through a 0.22 µm filter using a sterile 1 mL syringe. Extracts were immediately aliquoted per 20 µL, frozen and stored at -80°C.

Assay with usage of excretory-secretory (ES) metabolites containing ascarosides

Approx. 40 animals were transferred to 60 mm NGM plates seeded with *E. coli* HT115 immediately after hatching. Then, 40 µL of excretory-secretory metabolites were applied on the bacterial lawn and wrapped with parafilm right afterwards. In control plates, water was used instead. Worms' synchronous growth was monitored at the L4 stage when an additional 20 µL of ES metabolites or water was administered.

Generation of *str-173* mutant strains

The *str-173* gene mutants (*str-173(wwa1)* and *str-173(wwa2)*) were generated using CRISPR/Cas9 method as previously described[50]. The crRNA sequence used was ATAATTGGTGGATATACAAATGG. The *str-173* gene locus was sequenced and deletions were mapped to the first exon (Extended Data Figure 3d). Both mutations cause frame shifts, therefore, are most likely molecular null alleles.

Generation of optogenetic strains

Optogenetic strains created for this paper contain red-shifted Channel Rhodopsin (ReaChR) or archaerhodopsin from Halorubrum strain TP009 (ArchT). To generate these strains, firstly, mKate2-unc-54 3'UTR was amplified from the template and cloned into pCG150 to create pAZ03 plasmid. Next, *gcy-36* promoter was amplified from pMH389, ReaChR and ArchT were amplified from respective templates. The *gcy-36* promoter was then cloned into pAZ03 plasmid with ReaChR and ArchT separately. As a result two plasmids were created: gcy-36 promoter::ReaChR::mKate2-unc-54 3'UTR in pCG150 and gcy-36 promoter::ArchT::mKate2-unc-54 3'UTR in pCG150. To verify the correct sequence of the cloned constructs, plasmids were sequenced. All constructs generated for this study were made using the SLiCE method[51].

Transgenic strains with extrachromosomal arrays were generated by microinjection. DNA was injected into exopher reporter strain worms with muscle exopher RFP and mitochondrial GFP marker (ACH93). For injection, DNA was prepared as follows: construct 90 ng/µL and co-injection marker 10 ng/µL. Positive transformants were selected according to the presence of co-injection markers (myo-2 promoter::mNeonGreen).

The constructs created for this project and primers used for amplification are listed in the table at the beginning of the "Materials and Methods" section.

Optogenetics assay

For optogenetic activation or inhibition, 35-mm NGM plates seeded with HT115 *E. coli* bacteria were covered with 0.2 µM all-trans retinal (ATR). Control plates were not covered with ATR. Ten age-synchronized worms from optogenetic strains (expressing ReaChR or ArchT in AQR/PQR/URX neurons) were picked per plate at adulthood day 1. After 24-hour incubation at 20°C and darkness, muscle exophers extruded by worms were counted. Next, experimental plates were placed on the stereomicroscope and illuminated for 1 hour with green light (HXP 200C illuminator as a light source, band-pass filter Zeiss BP 572/25 (HE), the green light intensity measured at 561 nm = 0.07 mW/mm^2). Immediately after illumination muscle exophers were counted. Subsequently, exophers scorings were performed in 15 minutes intervals, and worms were kept in the darkness in between counts. The control group was not illuminated. To provide similar environmental conditions control plates were placed next to the experimental plate but shielded from light. Control and treated groups were randomized before the start of the experiment.

FUdR assay

584 Age-synchronized young adult animals (day 0) were placed on NGM plates containing 25 μM
585 fluorodeoxyuridine (FUdR) or control NGM plates without FUdR. Exophers number were
586 scored when worms reached adulthood day 2 using a stereomicroscope.

587 **Transcriptome analysis**

588 RNA extractions, library preparations, and sequencing were conducted at Azenta US, Inc
589 (South Plainfield, NJ, USA) as follows:

590 *RNA Extraction*

591 Total RNA was extracted using Qiagen RNeasy Plus mini kit following the manufacturer's
592 instructions (Qiagen, Hilden, Germany).

593 *Library Preparation with polyA selection and Illumina Sequencing*

594 Extracted RNA samples were quantified using Qubit 2.0 Fluorometer (Life Technologies,
595 Carlsbad, CA, USA) and RNA integrity was checked using Agilent TapeStation 4200 (Agilent
596 Technologies, Palo Alto, CA, USA).

597 RNA sequencing libraries were prepared using the NEBNext Ultra II RNA Library Prep Kit
598 for Illumina following the manufacturer's instructions (NEB, Ipswich, MA, USA). Briefly,
599 mRNAs were first enriched with Oligo(dT) beads. Enriched mRNAs were fragmented for 15
600 minutes at 94 °C. First strand and second strand cDNAs were subsequently synthesized. cDNA
601 fragments were end repaired and adenylated at 3'ends, and universal adapters were ligated to
602 cDNA fragments, followed by index addition and library enrichment by limited-cycle PCR.
603 The sequencing libraries were validated on the Agilent TapeStation (Agilent Technologies,
604 Palo Alto, CA, USA), and quantified by using Qubit 2.0 Fluorometer (Invitrogen, Carlsbad,
605 CA) as well as by quantitative PCR (KAPA Biosystems, Wilmington, MA, USA).

The sequencing libraries were multiplexed and loaded on the flowcell on the Illumina NovaSeq 6000 instrument according to the manufacturer's instructions. The samples were sequenced using a 2x150 Pair-End (PE) configuration v1.5. Image analysis and base calling were conducted by the NovaSeq Control Software v1.7 on the NovaSeq instrument. Raw sequence data (.bcl files) generated from Illumina NovaSeq was converted into fastq files and de-multiplexed using Illumina bcl2fastq program version 2.20. One mismatch was allowed for index sequence identification.

Sequencing Data Analysis

After investigating the quality of the raw data, sequence reads were trimmed to remove possible adapter sequences and nucleotides with poor quality using Trimmomatic v.0.36. The trimmed reads were mapped to the *Caenorhabditis elegans* reference genome available on ENSEMBL using the STAR aligner v.2.5.2b. The STAR aligner is a splice aligner that detects splice junctions and incorporates them to help align the entire read sequences. BAM files were generated as a result of this step. Unique gene hit counts were calculated by using feature Counts from the Subread package v.1.5.2. Only unique reads that fell within exon regions were counted.

After the extraction of gene hit counts, the gene hit counts table was used for downstream differential expression analysis. Using DESeq2, a comparison of gene expression between the groups of samples was performed. The Wald test was used to generate p-values and Log2 fold changes. Genes with adjusted p-values < 0.05 and absolute log2 fold changes > 1 were called as differentially expressed genes for each comparison.

Data analysis and visualization tools

The exophers were scored at adulthood day 2 using a stereomicroscope unless stated otherwise. Data analysis was performed using Microsoft® Excel® and GraphPad Prism 9 software. Graphical representation of data was depicted using GraphPad Prism 9.

Statistical analysis

No statistical methods were used to predetermine the sample size. Worms were randomly allocated to the experimental groups for all the data sets and experiments were performed blinded for the data sets presented in the following figures: Fig. 2b, e, f, h; Fig. 3b, c, f; Fig. 4f; Extended Data Fig. 3d, e, f. Non-Gaussian distribution of residuals was assumed and therefore nonparametric statistical tests were applied: Mann–Whitney (in comparison between two groups) or Kruskal-Wallis test with Dunn's multiple comparisons test (in comparison between more than two groups). *P*-value < 0.05 is considered significant**.**

References

1. Théry, C. *et al.* Minimal information for studies of extracellular vesicles 2018 (MISEV2018): a position statement of the International Society for Extracellular Vesicles and update of the MISEV2014 guidelines. *J. Extracell. Vesicles* **7**, 1535750 (2018).

2. Colombo, M., Raposo, G. & Théry, C. Biogenesis, Secretion, and Intercellular Interactions of Exosomes and Other Extracellular Vesicles. *Annu. Rev. Cell Dev. Biol.* **30**, 255–289 (2014).

3. Fu, S. *et al.* Extracellular vesicles in cardiovascular diseases. *Cell Death Discov.* **6**, 68 (2020).

4. Hill, A. F. Extracellular Vesicles and Neurodegenerative Diseases. *J. Neurosci.* **39**, 9269 LP – 9273 (2019).

5. Kalluri, R. The biology and function of exosomes in cancer. *J. Clin. Invest.* **126**, 1208–1215 (2016).

6. Wang, J. *et al.* C. elegans Ciliated Sensory Neurons Release Extracellular Vesicles that Function in Animal Communication. *Curr. Biol.* **24**, 519–525 (2014).

7. Melentijevic, I. *et al.* C. elegans neurons jettison protein aggregates and mitochondria under neurotoxic stress. *Nature* **542**, 367–371 (2017).

8. Turek, M. *et al.* Muscle-derived exophers promote reproductive fitness. *EMBO Rep.* e52071 (2021) doi:10.15252/embr.202052071.

9. Liégeois, S., Benedetto, A., Michaux, G., Belliard, G. & Labouesse, M. Genes required for osmoregulation and apical secretion in Caenorhabditis elegans. *Genetics* **175**, 709–724 (2007).

10. Kosinski, M., McDonald, K., Schwartz, J., Yamamoto, I. & Greenstein, D. C. elegans sperm bud vesicles to deliver a meiotic maturation signal to distant oocytes.

Development **132**, 3357–3369 (2005).

11. Cohen, J. D. *et al.* A multi-layered and dynamic apical extracellular matrix shapes the vulva lumen in Caenorhabditis elegans. *Elife* **9**, e57874 (2020).

12. Cooper, J. F., Guasp, R. J., Arnold, M. L., Grant, B. D. & Driscoll, M. Stress increases in exopher-mediated neuronal extrusion require lipid biosynthesis, FGF, and EGF RAS/MAPK signaling. *Proc. Natl. Acad. Sci.* **118**, e2101410118 (2021).

13. Nicolás-Ávila, J. A. *et al.* A Network of Macrophages Supports Mitochondrial Homeostasis in the Heart. *Cell* **183**, 94-109.e23 (2020).

14. Wong, S. S., Yu, J., Schroeder, F. C. & Kim, D. H. Population Density Modulates the Duration of Reproduction of C. elegans. *Curr. Biol.* **30**, 2602-2607.e2 (2020).

15. Perez, M. F. *et al.* Neuronal perception of the social environment generates an inherited memory that controls the development and generation time of C. elegans. *Curr. Biol.* **31**, 4256-4268.e7 (2021).

16. Wasson, J. A. *et al.* Neuronal control of maternal provisioning in response to social cues. *Sci. Adv.* **7**, (2021).

17. Brenner, S. The genetics of Caenorhabditis elegans. *Genetics* **77**, 71–94 (1974).

18. Kamath, R. S., Martinez-Campos, M., Zipperlen, P., Fraser, A. G. & Ahringer, J. Effectiveness of specific RNA-mediated interference through ingested double-stranded RNA in Caenorhabditis elegans. *Genome Biol.* **2**, RESEARCH0002 (2001).

19. Hodgkin, J., Horvitz, H. R. & Brenner, S. Nondisjunction Mutants of the Nematode CAENORHABDITIS ELEGANS. *Genetics* **91**, 67–94 (1979).

20. Ludewig, A. H. & Schroeder, F. C. Ascaroside signaling in C. elegans. *WormBook* 1–22 (2013) doi:10.1895/wormbook.1.155.1.

21. Kaplan, F. *et al.* Ascaroside expression in Caenorhabditis elegans is strongly dependent on diet and developmental stage. *PLoS One* **6**, e17804 (2011).

689 22. Ferkey, D. M., Sengupta, P. & L'Etoile, N. D. Chemosensory signal transduction in
690 Caenorhabditis elegans. *Genetics* **217**, iyab004 (2021).
691 23. Perkins, L. A., Hedgecock, E. M., Thomson, J. N. & Culotti, J. G. Mutant sensory cilia
692 in the nematode Caenorhabditis elegans. *Dev. Biol.* **117**, 456–487 (1986).
693 24. Schwartz, H. T. & Horvitz, H. R. The C. elegans protein CEH-30 protects male-
694 specific neurons from apoptosis independently of the Bcl-2 homolog CED-9. *Genes*
695 *Dev.* **21**, 3181–3194 (2007).
696 25. Srinivasan, J. *et al.* A blend of small molecules regulates both mating and development
697 in Caenorhabditis elegans. *Nature* **454**, 1115–1118 (2008).
698 26. Macosko, E. Z. *et al.* A hub-and-spoke circuit drives pheromone attraction and social
699 behaviour in C. elegans. *Nature* **458**, 1171–1175 (2009).
700 27. Qian, K.-Y. *et al.* Male pheromones modulate synaptic transmission at the C. elegans
701 neuromuscular junction in a sexually dimorphic manner. *Elife* **10**, e67170 (2021).
702 28. Aprison, E. Z. & Ruvinsky, I. Counteracting Ascarosides Act through Distinct
703 Neurons to Determine the Sexual Identity of C. elegans
704 Pheromones. *Curr. Biol.* **27**, 2589-2599.e3 (2017).
705 29. Biron, D., Wasserman, S., Thomas, J. H., Samuel, A. D. T. & Sengupta, P. An
706 olfactory neuron responds stochastically to temperature and modulates Caenorhabditis
707 elegans thermotactic behavior. *Proc. Natl. Acad. Sci.* **105**, 11002–11007 (2008).
708 30. Kuhara, A. *et al.* Temperature Sensing by an Olfactory Neuron in a Circuit Controlling
709 Behavior of C. elegans. *Science (80-.).* **320**, 803–807 (2008).
710 31. Byerly, L., Cassada, R. C. & Russell, R. L. The life cycle of the nematode
711 Caenorhabditis elegans. I. Wild-type growth and reproduction. *Dev. Biol.* **51**, 23–33
712 (1976).
713 32. Robertson, H. M. & Thomas, J. H. The putative chemoreceptor families of C. elegans.

WormBook 1–12 (2006) doi:10.1895/wormbook.1.66.1.

33. Gruner, M. *et al.* Feeding state, insulin and NPR-1 modulate chemoreceptor gene expression via integration of sensory and circuit inputs. *PLoS Genet.* **10**, e1004707 (2014).

34. Ryan, D. A. *et al.* Sex, Age, and Hunger Regulate Behavioral Prioritization through Dynamic Modulation of Chemoreceptor Expression. *Curr. Biol.* **24**, 2509–2517 (2014).

35. Wexler, L. R., Miller, R. M. & Portman, D. S. C. elegans Males Integrate Food Signals and Biological Sex to Modulate State-Dependent Chemosensation and Behavioral Prioritization. *Curr. Biol.* **30**, 2695-2706.e4 (2020).

36. McLachlan, I. G. *et al.* Diverse states and stimuli tune olfactory receptor expression levels to modulate food-seeking behavior. *Elife* **11**, (2022).

37. Taylor, S. R. *et al.* Molecular topography of an entire nervous system. *Cell* **184**, 4329-4347.e23 (2021).

38. White, J. G., Southgate, E., Thomson, J. N. & Brenner, S. The structure of the nervous system of the nematode Caenorhabditis elegans. *Philos. Trans. R. Soc. London. Ser. B, Biol. Sci.* **314**, 1–340 (1986).

39. Coates, J. C. & de Bono, M. Antagonistic pathways in neurons exposed to body fluid regulate social feeding in Caenorhabditis elegans. *Nature* **419**, 925–929 (2002).

40. Okazaki, A. & Takagi, S. An optogenetic application of proton pump ArchT to C. elegans cells. *Neurosci. Res.* **75**, 29–34 (2013).

41. Lin, J. Y., Knutsen, P. M., Muller, A., Kleinfeld, D. & Tsien, R. Y. ReaChR: a red-shifted variant of channelrhodopsin enables deep transcranial optogenetic excitation. *Nat. Neurosci.* **16**, 1499–1508 (2013).

42. Aprison, E. Z., Dzitoyeva, S., Angeles-Albores, D. & Ruvinsky, I. A male pheromone

that improves the quality of the oogenic germline. *Proc. Natl. Acad. Sci. U. S. A.* **119**, e2015576119 (2022).

43. Aprison, E. Z. & Ruvinsky, I. Sexually Antagonistic Male Signals Manipulate Germline and Soma of C. elegans Hermaphrodites. *Curr. Biol.* **26**, 2827–2833 (2016).

44. Corrigan, L. *et al.* BMP-regulated exosomes from Drosophila male reproductive glands reprogram female behavior. *J. Cell Biol.* **206**, 671–688 (2014).

45. Sanchez-Lopez, J. A. *et al.* Male-female communication enhances release of extracellular vesicles leading to high fertility in Drosophila. *Commun. Biol.* **5**, 815 (2022).

46. Berumen Sánchez, G., Bunn, K. E., Pua, H. H. & Rafat, M. Extracellular vesicles: mediators of intercellular communication in tissue injury and disease. *Cell Commun. Signal.* **19**, 104 (2021).

47. Roh, D. *et al.* The association between olfactory dysfunction and cardiovascular disease and its risk factors in middle-aged and older adults. *Sci. Rep.* **11**, 1248 (2021).

48. Liu, B. *et al.* Relationship Between Poor Olfaction and Mortality Among Community-Dwelling Older Adults: A Cohort Study. *Ann. Intern. Med.* **170**, 673–681 (2019).

49. Kamath, R. S. & Ahringer, J. Genome-wide RNAi screening in Caenorhabditis elegans. *Methods* **30**, 313–321 (2003).

50. Dokshin, G. A., Ghanta, K. S., Piscopo, K. M. & Mello, C. C. Robust Genome Editing with Short Single-Stranded and Long, Partially Single-Stranded DNA Donors in Caenorhabditis elegans. *Genetics* **210**, 781–787 (2018).

51. Zhang, Y., Werling, U. & Edelmann, W. SLiCE: a novel bacterial cell extract-based DNA cloning method. *Nucleic Acids Res.* **40**, e55–e55 (2012).

Acknowledgements

Some strains were provided by the CGC, which is funded by NIH Office of Research Infrastructure Programs (P40 OD010440). We thank Henrik Bringmann and Lukas Kapitein for plasmids; Frank Schroeder for expert advice; Peter Askjaer, Henrik Bringmann, and Antonio Miranda Vizuete for discussions and comments on the manuscript; Zofia Olszewska, Marta Niklewicz, and Monika Woźniak for assistance with worms maintenance. Work in the M. T. Laboratory was mainly funded by a National Science Centre SONATA grant (2019/35/D/NZ3/04091) and additionally supported by a National Science Centre SONATA BIS grant (2021/42/E/NZ3/00358). Work in the W. P. Laboratory was funded by the Foundation for Polish Science co-financed by the European Union under the European Regional Development Fund (grant POIR.04.04.00-00-5EAB/18-00 to K.B., and W.P.), and additionally supported by the European Molecular Biology Organization (EMBO Installation Grant No. 3916 to K.B., and W.P.), and the Norwegian Financial Mechanism 2014-2021 operated by the Polish National Science Centre, Poland (project contract number 2019/34/H/NZ3/00691 to W.P.).